

1  
2  
3  
4  
5  
6  
7  
8  
9  
10  
11  
12  
13  
14  
15  
16  
17  
18  
19  
20  
21  
22  
23  
24

# Investigating the effect of ballasting by $\text{CaCO}_3$ in *Emiliana huxleyi*:

## II. Decomposition of particulate organic matter

Anja Engel<sup>1,2</sup>, Lynn Abramson<sup>2</sup>, Jennifer Szlosek<sup>2</sup>, Zhanfei Liu<sup>2</sup>, Gillian Stewart<sup>2,3</sup>,  
David Hirschberg<sup>2</sup> and Cindy Lee<sup>2</sup>

<sup>1</sup> Present address: Alfred Wegener Institute for Polar and Marine Research, 27515  
Bremerhaven, Germany

<sup>2</sup> Marine Sciences Research Center, Stony Brook University, Stony Brook, NY 11794-  
5000, USA

<sup>3</sup> Present address: Earth and Environmental Sciences, Queens College, CUNY,  
Flushing, NY 11367, USA

---

<sup>1</sup>To whom correspondence should be addressed.

25 **Abstract**

26           The quantitative relationship between organic carbon and mineral contents of particles  
27 sinking below 1800 m in the ocean indicate that organisms with mineral shells such as  
28 coccolithophores are of special importance for transporting carbon into the deep sea. Several  
29 hypotheses about the mechanism behind this relationship between minerals and organic  
30 matter have been raised, such as mineral protection of organic matter or enhanced sinking  
31 rates through ballast addition. We examined organic matter decomposition of calcifying and  
32 non-calcifying *Emiliana huxleyi* cultures in an experiment that allowed aggregation and  
33 settling in rotating tanks. Biogenic components such as particulate carbon, particulate  
34 nitrogen, particulate volume, pigments, transparent exopolymer particles (TEP) and  
35 particulate amino acids in suspended particles and aggregates were followed over a period of  
36 30 days. The overall pattern of decrease in organic matter, the amount of recalcitrant organic  
37 matter left after 30 days, and the compositional changes within particulate organic matter  
38 indicated that cells without a shell are more subject to loss than calcified cells. It is suggested  
39 that biogenic calcite helps in the preservation of POM by offering structural support for  
40 organic molecules. Over the course of the experiment, half the particulate organic carbon in  
41 both calcifying and non-calcifying cultures was partitioned into aggregates and remained so  
42 until the end of the experiment. The partial protection of particulate organic matter from  
43 solubilization by biominerals and by aggregation that was observed in our experiment may  
44 help explain the robustness of the relationship between organic and mineral matter fluxes in  
45 the deep ocean.

46

47 **Keywords: Ballast, coccolithophores, degradation, aggregation, PCA, TEP**

48

49

## 50           **1. Introduction**

51   Recent findings suggest that the ratio of minerals, i.e., opal (biogenic silica), calcium  
52   carbonate, and quartz, to organic carbon (Min.:Corg) provides a means of understanding  
53   export fluxes of organic matter (OM) to the deep ocean (Armstrong et al., 2002; Francois et  
54   al., 2002; Klaas and Archer, 2002). This is based on the analysis of field data showing that  
55   the Min:Corg ratio in particulate matter is generally constant below a depth of 1800m. There  
56   are several mechanisms that might cause such a relationship (Hedges and Keil, 1995;  
57   Armstrong et al., 2002; Klaas and Archer, 2002). First, organic compounds may be  
58   physically protected against microbial degradation by their association with minerals. In  
59   addition, OM may glue particles together, forming aggregates; if the particulate organic  
60   carbon content becomes too low, particles may disintegrate, removing both POC and minerals  
61   from observed fluxes. Or, the settling velocity of particles may increase when associated with  
62   more dense mineral material, leading to a faster export of the ballasted OM (Smayda, 1970;  
63   McCave, 1975; Ittekkot and Haake, 1990). Whereas the role of minerals in the preservation of  
64   OM has been studied extensively in marine sediments (Suess, 1973; Hedges and Keil, 1995;  
65   Mayer 2004) and in soils (see review in Baldock and Skjemstad, 2000), only little is known  
66   about the effect of biologically produced minerals on the decomposition rates of settling OM  
67   during its transit through the water column. OM in seawater becomes associated with  
68   minerals through adsorption onto mineral surfaces, aggregation with clay sized particles or  
69   biologically by growth of cells that produce an outer mineral shell (e.g., the opal frustules of  
70   diatoms and radiolaria or calcium carbonate shells of foraminifera, pteropods and  
71   coccolithophores). Comparing the carrying capacity of different minerals, i.e., the organic  
72   carbon fraction associated with the mineral, Klaas and Archer (2002) showed that CaCO<sub>3</sub> and  
73   lithogenic material are more efficient than opal in the downward transport of organic carbon.  
74   The special role of CaCO<sub>3</sub> in chemical and physical protection of OM in soils has been

75 summarized in Baldock and Skjemstad (2000). It is suggested that  $\text{Ca}^{2+}$  cations aid in the  
76 preservation of OM by the formation of Ca-organic linkages (Duchaufour, 1976). These  
77 linkages can alter the structure of organic macromolecules and the orientation of functional  
78 groups, with likely implications for the efficiency of enzymatic attack (Oades, 1988).  
79 Stabilization of OM by  $\text{CaCO}_3$  during export to the deeper ocean will have large implications  
80 for understanding the ocean's capacity to store  $\text{CO}_2$  and therefore needs to be included in  
81 numerical modeling that aims to quantify the marine carbon cycle. Moreover, since recent  
82 investigations have shown a decrease in biogenic calcification with ocean acidification  
83 (Riebesell et al., 1993; Delille et al., 2004), understanding the relationship between calcite and  
84 OM preservation will also be important to predict future changes in OM decomposition.

85

86 To investigate the effect of biogenic  $\text{CaCO}_3$  on the preservation of and ballasting of  
87 OM, we compared the formation and settling velocities of aggregates (Engel et al., 2008) as  
88 well as the decomposition of POM during laboratory incubations of a non-calcifying and a  
89 calcifying strain of the marine coccolithophore *Emiliana huxleyi*. Here, we report the changes  
90 in the chemistry of dissolved and particulate components during microbial decomposition and  
91 discuss the role of calcification for the preservation of OM. *E. huxleyi* is a widespread,  
92 bloom-forming coccolithophore in the ocean that participates in the export of calcite and  
93 organic matter to the deep sea. Since aggregates rather than single cells are the most likely  
94 carriers of particle flux in the deep ocean (Fowler and Knauer, 1986), we allowed cells to  
95 aggregate prior to and during the experiment and analyzed suspended and aggregated particles  
96 separately.

97

98

99

## 100           **2. Materials and Methods**

101           **A list of abbreviations is given in table 1.**

### 102           2.1 Experimental set-up

103           Decomposition of calcifying (CAL) and non-calcifying (NCAL) *Emiliana huxleyi*  
104 cells were compared under conditions that allowed aggregation and settling of the cells as  
105 similar as possible to what might occur in the water column (Fig. 1). Non-calcifying and  
106 calcifying strains of the coccolithophore *E. huxleyi* were grown in batch culture at 15°C and  
107 salinity 35.1 with a light flux of 100  $\mu\text{mol m}^{-2} \text{s}^{-1}$  in a 16h: 8h light: dark cycle. Seventy liters  
108 of each culture were grown in f/4 media (Guillard, 1975) (initial  $[\text{NO}_3]$ : 265  $\mu\text{mol L}^{-1}$ , initial  
109  $[\text{PO}_4]$ : 9.38  $\mu\text{mol L}^{-1}$ ). The pH of the cultures was initially adjusted to 7.5 to assure that  $\text{CO}_2$   
110 was abundant during growth. The cultures were aerated during the 16h light period. The  
111 purity of each culture (i.e., the predominance of calcifying or non-calcifying cells) was  
112 confirmed by microscopic observations at 1000x magnification.

113           Incubation of the two cultures (CAL and NCAL) in rotating tanks on roller tables was  
114 performed in series, not in parallel. When each culture reached late exponential growth  
115 phase, it was transferred to 7 tanks of 4.5-L volume each and kept in the dark at 9°C. To  
116 promote aggregation of cells, all tanks were placed on roller tables (Shanks and Edmondson,  
117 1989) that rotated at 0.66 rpm. To simulate the sinking of aggregates into deeper and more  
118 dilute waters, the particle concentration was lowered before the decomposition experiment  
119 began. This was accomplished by removing tanks from the roller table after 5 days and  
120 allowing particles to settle for 10 minutes. Then 3L of supernatant were removed from each  
121 tank and replaced coastal seawater taken at the Long Island Sound and aged for 2 months in  
122 the dark at 9°C. At this point, the tanks were again placed on roller tables rotating at 0.66 rpm,  
123 and the incubation begun (i.e., time zero corresponds to the time at which the supernatant was  
124 replaced by filtered seawater). To prevent collision between aggregates and the tank wall, the

125 rotation speed was repeatedly increased during the experiment respectively. At each sampling  
126 point one tank was harvested. Each experiment lasted for 30 days with 7 sampling points  
127 (days 0, 3, 6, 10, 16, 23, 30).

128

## 129 2.2 Sampling

130 Aggregates and suspended particles without aggregates ( $< 1\text{mm}$ ) were analyzed  
131 separately. On each sampling day, one 4.5 L tank was removed from the roller table and  
132 turned on its sides for 20 minutes, allowing particles to settle to the bottom. Then the upper  
133 lid of the tank was removed and 2x 200ml of seawater was drained through a Tygon tube by  
134 gravity into glass bottles for immediate determination of pH and  $\text{O}_2$  concentration.

135 Aggregates, i.e. particles  $\geq 1\text{ mm}$  that settled to the bottom of the tank within 20 minutes and  
136 were large enough to be clearly identified as aggregates, were carefully removed from the  
137 bottom of the tank with as little surrounding seawater as possible using a 10-mL serological  
138 pipet and mild suction. The volume of several aggregates at a time was determined to the  
139 nearest 0.1 mL inside the pipette, and these particles transferred to a Nalgene bottle. This  
140 process was repeated until all aggregates in the tank were removed, yielding a pooled  
141 aggregate sample for each tank containing about 20-50 aggregates for NCAL and 50-200  
142 aggregates for CAL at each day of sampling. The total volume of the pooled aggregate  
143 sample per tank water was calculated. Three-hundred mL of 0.2- $\mu\text{m}$  filtered seawater were  
144 added to the bottle, and the aggregates disaggregated by gentle agitation. Aliquots were  
145 removed from the bottle for various analyses.

146 The pooled aggregate sample contained aggregates as well as some surrounding  
147 seawater (SUSP) that is inevitably collected together with the aggregates. While the volume  
148 fraction of SUSP in the pooled slurry was assumed to be larger than the volume fraction of  
149 collected aggregates, particle concentration within aggregates is enriched by generally 2-4

150 orders of magnitude. To obtain a conservative estimate of concentrations within aggregates,  
151 the concentrations of particulate components in the SUSP were subtracted from those in the  
152 slurry. This corrected aggregate sample (AGG) is hence considered to be a representative  
153 average of just aggregates within the tank. AGG concentrations reported here for each  
154 component are per liter of tank water. Subsamples of SUSP were collected from tank water  
155 after aggregates had been removed in order to determine particulate components therein. The  
156 total volume of tank water was determined using a 1000 ml graduated cylinder.

157

### 158 2.3 Biological and chemical analysis

159 The pH of tank water was determined with an Orion perPHect LogRmeter (model  
160 370). Dissolved oxygen was measured with a YSI oxygen meter (Model 55). Alkalinity was  
161 calculated from temperature and pH according to Parsons et al. (1984). Ambient carbonate ion  
162 concentration was calculated using the CO<sub>2</sub>sys-software developed by Lewis and Wallace  
163 (1998), measured pH, temperature and alkalinity data, and the calculation scheme of Peng et  
164 al. (1987), and the dissolution constants of Mehrbach et al. (1973).

165 Particulate mass was determined by gently (200 mbar) filtering 400-600 mL tank  
166 water (SUSP) and 60-80 mL AGG slurries onto combusted, pre-weighed GF/F filters, oven  
167 drying the filters at 60°C for 24 h, and reweighing. Total particulate carbon (TPC),  
168 particulate organic carbon (POC) and particulate organic nitrogen (PN) were determined by  
169 elemental analysis from 50-200 mL tank water (SUSP) and 20-50 mL AGG samples filtered  
170 gently through combusted (24 h, 500°C) GF/F (Whatman) filters. For determination of POC,  
171 filters were fumed for 2 h in air saturated with HCl to remove inorganic carbon, and dried for  
172 2 h at ca. 50°C. TPC, POC, and PN were subsequently measured on a CHN-analyzer (Carlo  
173 Erba EA-1100). All filters were prepared in duplicate and stored at -20°C until analysis.  
174 Particulate inorganic carbon (PIC) was determined by subtracting POC from TPC.

175 Chlorophyll-*a* was extracted from filters with acetone during 20 minutes of sonication  
176 and analyzed using high performance liquid chromatography (HPLC) using the method and  
177 apparatus described by Sun et al. (1991). Briefly, 100 mL tank water (SUSP) or 20 mL AGG  
178 samples were filtered onto combusted GF/F filters, which were extracted twice using 100%  
179 acetone. The extracts were combined and filtered through a 0.2- $\mu$ m Zetapor membrane.  
180 Samples were injected within 24 hours of extraction onto a 5- $\mu$ m Adsorbosphere C-18 HPLC  
181 column and separated as described by Mantoura and Llewellyn (1983) and Bidigare et al.  
182 (1985). Chl *a* retention time and concentrations were determined using an authentic standard  
183 (Turner Design). Duplicate analyses of the samples agreed within 30%.

184 Total hydrolyzable amino acids were analyzed by fluorescence HPLC after acid hydrolysis  
185 according to Lee and Cronin (1982, 1984) and Lee et al. (2000). Either 50-100 mL tank water  
186 (SUSP) or 10-20 mL AGG samples were filtered onto combusted GF/F filters. The filters  
187 were sealed under N<sub>2</sub> in glass vials containing 6N HCl with 0.25 wt% phenol and hydrolyzed  
188 at 110°C for 20h. Hydrolyzates were filtered through 0.2- $\mu$ m disposable cellulose acetate  
189 syringe filters to remove particulates, evaporated under N<sub>2</sub>, and dissolved in Milli-Q water.  
190 Amino acids were then analyzed by HPLC following derivatization with o-phthaldialdehyde  
191 (OPA) after Lindroth and Mopper (1979) using an Alltech Altima C-18 250-mm 5- $\mu$ m  
192 column. OPA-derivatized amino acids were detected by fluorescence and identified by  
193 comparison to the retention times of amino acids in a standard mixture (Pierce Chemical  
194 Standard H with the non-protein amino acids  $\beta$ -alanine and  $\gamma$ -aminobutyric acid added).  
195 Duplicate analyses of the samples generally agreed within 30%.

196 Particle concentration, volume and size distribution of both AGG and SUSP between  
197 2 and 60  $\mu$ m equivalent spherical diameter (ESD) were determined using a Coulter Counter  
198 (Coulter Multisizer II) from replicate 2-mL samples. Samples were diluted by a factor of 10-  
199 20 with 0.2- $\mu$ m filtered seawater to keep coincidence of particles entering the aperture <5%.

200            Transparent Exopolymer Particles (TEP) were detected by staining with Alcian Blue,  
201 a cationic copper phthalocyanine dye that complexes carboxyl and half-ester sulfate reactive  
202 groups of acidic polysaccharides. The amount of Alcian Blue adsorption per sample volume  
203 is a measure of TEP concentration and was determined colorimetrically according to Passow  
204 and Alldredge (1995) from 20-30 mL tank water (SUSP) or 5-10 mL AGG samples filtered  
205 onto 0.4- $\mu\text{m}$  Nuclepore filters. All filters were measured in triplicate. The concentration of  
206 TEP is given in carbon units using a conversion factor of 0.325 mol C/g xanthan gum  
207 equivalent (Xeq.) as determined for *E. huxleyi* by Engel et al. (2004). Engel et al. (2004)  
208 previously showed that adsorption of stain to the cell surface of calcifying *E. huxleyi* was  
209 equivalent to 0.085 pmol C cell<sup>-1</sup>. Thus, for the calcifying strain used during this experiment,  
210 the total amount of TEP was corrected for the amount of Alcian Blue adsorbed by the cell.  
211 The calcified cell corrected amount of TEP was thus calculated by subtracting  $1.02 \times 10^{-12}$  g C  
212 cell<sup>-1</sup> times the number of cells present from the observed amount of TEP (g Xeq. L<sup>-1</sup>). Cell  
213 abundance was determined using a Coulter Counter (Multisizer II).

214            For determination of bacterial abundance, SUSP and AGG samples were preserved in  
215 4% (final conc.) formaldehyde at room temperature in the dark for about 4 months until  
216 analysis. Ten ml of SUSP and 1 ml of diluted AGG samples were filtered onto black 0.2- $\mu\text{m}$   
217 polycarbonate membrane filters (Nuclepore) and stained with pre-filtered (0.2  $\mu\text{m}$ ) 0.01%  
218 acridine orange (AO) solution (Hobbie et al., 1977). The preserved AGG samples were  
219 diluted 1:10 with 0.2- $\mu\text{m}$  filtered seawater within 24 hours to prevent excessive cell overlap.  
220 Stained filters were mounted onto glass slides, covered with immersion oil and a glass  
221 coverslip, and frozen at  $-20^{\circ}\text{C}$ . Slides were then viewed at 1000 $\times$  magnification using an  
222 epifluorescence microscope (ZEISS Axioskop, blue excitation 450-490 nm). Direct counts  
223 were made on 10 to 20 randomly chosen grids (grid is 10- $\mu\text{m}$  long on each edge),  
224 corresponding to 500-1000 cells. These samples were intended for quantification of bacterial

225 cell volume. For this purpose, the fluorochrome AO was chosen over DAPI because the latter  
226 has been shown to underestimate average cell biovolume (Suzuki et al., 1993). For most  
227 samples, cell coverage on filters was patchy and background fluorescence was high. Thus,  
228 images for bacterial cell volume determination were not recorded because the weak contrast  
229 between cells and the background would contribute to high errors. Loss in cell fluorescence  
230 due to storage temperature was not accounted for (Turley and Hughes, 1994).

231

## 232 2.4 Data analysis

233 The rate constant of decay ( $k$ ,  $d^{-1}$ ) of each parameter was calculated assuming a first-  
234 order exponential decay model:  $C(t)=C(0)e^{-kt}$ , where  $C(t)$  is the concentration of the  
235 component at time  $t$  and  $C(0)$  is the concentration at time  $t(0)$ . The curve fit to the data was  
236 performed using the software package Sigma Plot 9.0 (SYSTAT). Comparison of decay rates  
237 or regression coefficients between CAL and NCAL were performed with  $t$ -tests.

238

239

### 240 2.4.1 Principal components analysis

241 Principal components analysis (PCA) is a multivariate regression analysis that can be  
242 used to elucidate compositional differences among samples in a data matrix. PCA is  
243 increasingly being used to analyze organic compound data sets to discriminate subtle  
244 difference between samples and to determine the extent of sample degradation (Dauwe and  
245 Middelburg, 1998; Dauwe et al., 1999; Sheridan et al., 2002; Ingalls et al., 2006). PCA  
246 normally reduces the number of variable to two major principal components, PC1 and PC2,  
247 which are regression lines passing through the center (mean) of the data along its maximum  
248 gradients. PC1 explains the largest source of variance in the data matrix, while PC2 explains  
249 the second-largest source of variance. Site scores are the relative positions of each sample

250 along each principal component axis, and reveal their distances from the origin of all the data  
251 (the mean sample). Loadings (eigenvectors) of each variable indicate that variable's  
252 contribution to the data variability along each principal component axis. Using Sirius 7.0  
253 (Pattern Recognition Systems), we performed principal component analysis on a data matrix  
254 that included amino acid and pigment composition (mole%) after standardization by  
255 subtracting the mean for each compound and dividing by its standard deviation.

256

257

### 258 **3. Results**

#### 259 3.1 Changes in dissolved constituents with time

260 Over the course of the experiment, organic matter was clearly lost from the particulate  
261 phase in experiments with both non-calcifying (NCAL) and calcifying (CAL) cultures, and at  
262 least part of this POC was decomposed to CO<sub>2</sub>. At t<sub>0</sub> the pH of tank seawater was 8.0 for  
263 NCAL and 7.8 for CAL cultures. Due to the decomposition of organic matter, pH decreased  
264 in both cultures during the experiment (not shown). Initial alkalinity in the non-calcifying  
265 culture averaged 1.89 mmol L<sup>-1</sup>. In CAL, alkalinity was reduced to 1.09 mmol L<sup>-1</sup> at t<sub>0</sub> due to  
266 biogenic calcification, but increased to 1.38 after 30 d indicating calcite dissolution. In both  
267 incubations, the tanks were saturated with dissolved oxygen at t<sub>0</sub>; initial O<sub>2</sub> concentrations  
268 were 256 μmol L<sup>-1</sup>. Apparent oxygen utilization (AOU) during the 30-d incubations was  
269 similar in both experiments, 92 μmol  
270 O<sub>2</sub> L<sup>-1</sup> for the NCAL and 97 μmol O<sub>2</sub> L<sup>-1</sup> for the CAL *E. huxleyi* cultures. The tanks did not  
271 become anoxic or even hypoxic at any point.

272

273

#### 274 3.2 Temporal changes in particulate constituents

275 Decomposition of particulate components revealed very clear first-order exponential  
276 decay patterns during both experiments from day 3 onwards (Table 2). During the CAL  
277 incubation an increase in concentration between day 0 and day 3 was observed for some  
278 components. The increase of biogenic components in enclosed systems, the so called ‘bottle  
279 effect’ (Zobel and Anderson, 1936), is well known and can lead to a fivefold increase in  
280 bacterial abundance (Ferguson et al., 1984). To compare maximum rates of organic matter  
281 degradation, we chose the data between day 3 (maximum value) and day 30 to calculate the  
282 decay rate ( $k$ ) of these components in both experiments. Decay rates of all particulate  
283 components studied were significantly different between the two experiments (Table 2).

284

### 285 3.2.1 Particulate Volume (PV)

286 Total (SUSP+AGG) cell abundance and total PV, i.e. the sum of volumes of all  
287 particulate components  $>2 \mu\text{m}$  as determined by the Coulter Counter, decreased over time in  
288 both experiments. Initially, total cell abundances in the tanks were  $2.66 \times 10^6 \text{mL}^{-1}$  for the non-  
289 calcifying (NCAL) and  $1.77 \times 10^6 \text{mL}^{-1}$  for the calcifying (CAL) culture; these concentrations  
290 decreased to 7% (NCAL) and 26% (CAL) of initial values after 30 d (data not shown). The  
291 average size of the calcifying *E. huxleyi* cells was  $4.2\text{-}\mu\text{m}$  equivalent spherical diameter  
292 (ESD), slightly larger than the average size of cells that lacked a coccosphere (ESD= $3.7 \mu\text{m}$ ).  
293 Due to the larger size of calcified cells, the total PV of both cultures were quite similar at  $t_0$   
294 (Fig. 2) despite the difference in cell concentrations. The extent of decrease in total PV  
295 during the course of incubation was significantly different for the two cultures ( $p < 0.001$ ).  
296 Within the first two weeks, total PV in the NCAL culture decreased by 81%, whereas only  
297 36% reduction of total PV was observed in the CAL culture. Rate constants of loss were  
298  $0.043 \pm 0.114 \text{d}^{-1}$  for CAL cultures and  $0.129 \pm 0.021 \text{d}^{-1}$  for NCAL (Table 2).

299

300           Aggregates became visible, i.e. larger than 0.5 mm, within the first hours of incubation  
301 in the CAL culture. Visible aggregation was delayed for 1 week in the tanks containing the  
302 NCAL culture. Details on formation, settling velocities and physical properties of aggregates  
303 during both incubations will be published elsewhere (Engel et al., 2007). PV in AGG,  
304 defined as the sum of volumes of particles  $>2 \mu\text{m}$  per AGG as determined by the Coulter  
305 Counter, was  $0.7 \mu\text{l L}^{-1}$  and  $0.04 \mu\text{l L}^{-1}$  at the onset of aggregate formation in the CAL (day 1)  
306 and NCAL (day 6) incubations, respectively. AGG PV increased to a maximum of  $3.4 \mu\text{l L}^{-1}$   
307 for  $\text{AGG}_{\text{CAL}}$  and  $1.3 \mu\text{l L}^{-1}$  for  $\text{AGG}_{\text{NCAL}}$ , equivalent to 30% (CAL) and 11 % (NCAL) of the  
308 initial total PV. The PV fraction contained in AGG, relative to the total PV on the same day,  
309 reached maximum values of 75% (CAL) and 72% % (NCAL). Hence, the major fraction of  
310 particles  $>2\mu\text{m}$  were contained in aggregates at the end of the experiment (Fig. 2).

311

### 312           3.2.2 Particulate carbon and nitrogen

313           Decomposition of total (AGG+SUSP) POC and PN was significantly larger in NCAL  
314 than in CAL ( $p<0.001$ ) (Table 2, Fig. 3). Initial total POC concentration in CAL was higher  
315 ( $606 \mu\text{mol L}^{-1}$ ) than in the NCAL ( $461 \mu\text{mol L}^{-1}$ ) and increased until day 3. Thereafter total  
316  $\text{POC}_{\text{CAL}}$  was decomposed to  $585 \mu\text{mol L}^{-1}$ , which is equivalent to 96% of the initial value.  
317 (Fig 3a). In the NCAL culture, the final concentration of total POC was  $273 \mu\text{mol L}^{-1}$ ,  
318 equivalent to 59% of the initial value.

319           In both,  $\text{AGG}_{\text{CAL}}$  and  $\text{AGG}_{\text{NCAL}}$ , POC concentration increased until day 10 and  
320 remained almost stable thereafter at values of  $193\pm 7.3 \mu\text{mol L}^{-1}$  for NCAL and  $262\pm 16 \mu\text{mol}$   
321  $\text{L}^{-1}$  for CAL, (Fig. 3a). The increase of POC in AGG followed a logarithmic growth function  
322 in both experiments with a correlation coefficient of  $r^2=0.980$  for CAL and  $r^2=0.997$  for  
323 NCAL, indicating a limitation on the aggregation process or a balance between aggregation  
324 and disaggregation, or between aggregation and aggregate decomposition respectively,

325 between days 10 and 30. The final amount of POC contained in AGG was about 42% of the  
326 initial total POC concentration in both experiments. However, related to total POC at the time  
327 of observation, the fraction of POC contained in AGG<sub>NCAL</sub> was about 70% and much higher  
328 than the 49% in AGG<sub>CAL</sub>.

329 Total particulate mass was initially 16.3 mg L<sup>-1</sup> in NCAL and more than two-times  
330 lower than CAL (42.2 mg L<sup>-1</sup>), which had coccolith forming cells. By the end of the  
331 experiment total particulate mass decreased by 27.3% in NCAL and by 16.9% in CAL (data  
332 not shown). Average POC:mass ratios for total particulates during the experiment were  
333 0.35±0.04 for NCAL and 0.17±0.03 for CAL. For NCAL, total POC: mass ratios did not  
334 change significantly over time, whereas a slight increase in this ratio was observed for CAL  
335 (p=0.011). POC:mass ratios for AGG<sub>NCAL</sub> were higher than for AGG<sub>CAL</sub> due to the higher  
336 mass of the coccosphere in the calcified cell and consistent with other bulk measurements.  
337 However, POC:mass ratios for AGG<sub>NCAL</sub> were higher than POC:mass ratios of total  
338 particulates in NCAL, indicating a selective enrichment of POC in AGG in the non-calcifying  
339 culture.

340 Total PIC concentration in CAL tanks increased until day 6, indicating ongoing  
341 coccolith formation, and fell continuously thereafter to about 20% of the initial value (data not  
342 shown). Due to the dissolution of PIC molar total PIC:POC ratios decreased from 0.7 initially  
343 to 0.1 at the end of the experiment. PIC:POC ratios in AGG<sub>CAL</sub> varied between 0.45 and 0.8,  
344 but in contrast to total PIC:POC ratios, showed no clear pattern over time. At the end of the  
345 experiment PIC:POC ratios were at least two times higher in AGG than in total particulates,  
346 indicating reduced PIC dissolution in AGG.

347

348 Initial total PN concentrations were about 50 µmol L<sup>-1</sup> in both experiments (Fig. 3b).  
349 PN concentrations increased from day 0 to day 3 in both tanks and decreased exponentially

350 thereafter. The rate of total PN decrease in NCAL was about three times higher than in CAL  
351 (Table 2), and yielded a final total PN concentration of  $22.9 \mu\text{mol L}^{-1}$ , equivalent to 45% of  
352 the initial value. In the CAL culture, PN concentration decreased to  $36.8 \mu\text{mol L}^{-1}$ , 75% of  
353 the initial value, again indicating very little decomposition during the 1-month incubation.  
354 Molar POC:PN ratios for all particulates (SUSP+AGG) were initially 9.1 for NCAL and 11.1  
355 for CAL and clearly above the Redfield C:N ratio of 6.6 (Redfield et al. 1963). In both  
356 experiments the ratio increased over time with the highest values at  $t=16$  of 14.2 and 15.9 for  
357 NCAL and CAL, respectively. Molar POC: PN in AGG varied from 12.2 to 15 for NCAL and  
358 from 8.9 to 17.7 for CAL.

359

### 360 3.2.3 Pigments

361 Total (SUSP+AGG) Chl *a* concentration was initially higher for CAL than for NCAL  
362 (Fig. 4). Ratios of the pigment decomposition products pheophytin (Pptn) and pheophorbide  
363 (Ppb) (Pptn + Ppb) to their precursor, Chl *a*, were very small (0.03) for both cultures initially,  
364 indicating the presence of fresh algal material at the beginning of both experiments. An  
365 exponential decay (note log scale in Fig. 4) of Chl *a* was observed during both experiments.  
366 with no initial increase in Chl *a* concentration at day 3. Decomposition of Chl *a* was  
367 significantly faster in NCAL than in CAL ( $p < 0.001$ , Table 2). Faster degradation of Chl *a* in  
368 NCAL was also indicated by a significantly steeper increase of the ratio of pheopigments  
369 (Pptn+Ppb)/Chl *a* during the NCAL experiment ( $p < 0.01$ ), yielding final ratios of 0.62 for  
370 NCAL and only 0.30 for CAL.

371 No significant difference in Chl *a* degradation was observed between the AGG  
372 fractions of NCAL and CAL (Fig. 4). For both cell types, however, the SUSP fractions  
373 exhibited significantly higher ratios of pheopigments to Chl *a* and faster increases in these

374 ratios than did their corresponding AGG fractions ( $t$ -test,  $p < 0.01$ , Fig. 4), indicating  
375 preferential decomposition of SUSP cells.

376 The ratio of Chl  $a$  to PN in AGG was  $0.28 \pm 0.03$  and  $1.48 \pm 0.56$  for NCAL and CAL  
377 respectively. These ratios were significantly higher than for SUSP with  $0.039 \pm 0.02$  (NCAL)  
378 and  $0.069 \pm 0.02$  (CAL) ( $t$ -test,  $p < 0.001$ ).

379

### 380 3.2.4 TEP and PAA

381 Initial total (SUSP+AGG) TEP concentrations were  $53.3$  and  $60.5 \mu\text{mol C L}^{-1}$  in the CAL and  
382 NCAL cultures, respectively (Fig. 5). On day 3, total TEP concentration in CAL increased  
383 sharply by 36% over the initial value, whereas no increase was observed in NCAL. Total  
384 TEP: POC (mol C: mol C) ratios were initially 0.088 and 0.131 for the CAL and NCAL  
385 culture, respectively. These values are relatively low when compared to TEP:POC ratios of  
386 0.38-0.55 observed during a mesocosm experiment with a bloom dominated by calcifying *E.*  
387 *huxleyi* (Engel et al., 2004). In both experiments, total TEP:POC ratios decreased  
388 significantly over the course of the experiment ( $p < 0.005$  for NCAL and CAL). No data were  
389 obtained for NCAL on day 6 due to a break down of the photometer during measurement.

390 The rate constant of total TEP decomposition was significantly higher in NCAL than in CAL  
391 experiments ( $p < 0.01$ ) (Table 2). In AGG, TEP concentration was initially  $17.9 \mu\text{mol C L}^{-1}$  for  
392 CAL and  $5.9 \mu\text{mol C L}^{-1}$  for NCAL (day 5). TEP concentration for AGG<sub>NCAL</sub> increased to a  
393 maximum of  $14.8 \mu\text{mol C L}^{-1}$  390 on day 23, while that for AGG<sub>CAL</sub> did not increase. The  
394 percentage of POC made up by TEP was 44% for AGG<sub>CAL</sub> initially and decreased to 3.9 % at  
395 the end of the experiment. In NCAL, the TEP contribution to POC in AGG was on average  
396  $3.6 \pm 1.2 \%$  with no significant changes over time. Accordingly, TEP:mass (g:g) ratios in  
397 aggregates did not change significantly for NCAL either and yielded an average value of  
398  $0.19 \pm 0.08 \%$ . In CAL incubations, TEP:mass (g:g) ratios decreased from 0.5% to 0.14%.

399  
400 Total particulate amino acid (PAA) concentrations were initially  $36.6 \mu\text{mol L}^{-1}$  and  $25.7 \mu\text{mol}$   
401  $\text{L}^{-1}$  for the CAL and NCAL, respectively. As for total PN, the total PAA concentration  
402 increased during both experiments on day 3 and decreased exponentially thereafter (Table 2,  
403 Fig. 6). After day 3, total PAA concentration decreased significantly faster in CAL ( $p < 0.01$ )  
404 (Table 2), to about 53% of the initial concentration. In NCAL cultures, about 60% of the  
405 initial concentration was left at the end of the experiment. However, no difference in the rate  
406 of total PAA decrease was observed when the data of day 3 were omitted. Using the nitrogen  
407 content of each amino acid determined, we calculated that at day 3, 96.6% of PN in CAL was  
408 contained in PAA. Such a high contribution of PAA to PN indicates the production of  
409 proteinaceous particles, such as bacteria (Fig. 7) and Coomassie Blue stainable particles  
410 (CSP) (Long and Azam, 1996), or adsorption of dissolved amino acids onto particles. Hence  
411 concentration pattern of PAA in CAL and NCAL during the first days of the experiment were  
412 likely due to a combination of algal decomposition, bacterial dynamics and adsorption/  
413 desorption processes. PAA in AGG<sub>CAL</sub> increased much faster than in AGG<sub>NCAL</sub>.

414

### 415 3.2.5 Bacteria

416 The total (SUSP+AGG) concentration of bacteria was initially  $2.0 \pm 6.0 \times 10^5 \text{ cell mL}^{-1}$   
417 and  $8.0 \pm 5.4 \times 10^5 \text{ cell mL}^{-1}$  in the NCAL and CAL cultures, respectively, and increased  
418 during both experiments by one order of magnitude. No significant differences in the bacteria  
419 concentration or the rate of increase of bacteria concentration between the two cultures were  
420 observed ( $t$ -test,  $p=0.28$ ) (Fig. 7). On day 16 very high bacteria concentrations were observed  
421 during both experiments in the SUSP as well as in the AGG fractions. Because these samples  
422 were filtered and analyzed on different dates a methodological error seems unlikely.

423 However, the increase of bacteria abundance at day 16 was not reflected in changes of other  
424 organic matter variables or oxygen consumption rates.

425 Bacteria in aggregates were enriched by two orders of magnitude relative to SUSP,  
426 yielding final concentrations of  $6.1 \pm 3.5 \times 10^8$  and  $3.0 \pm 1.6 \times 10^8$  cells mL<sup>-1</sup> AGG for the  
427 NCAL and CAL cultures, respectively. The percentage of bacteria in AGG varied between  
428 52 and 94% of total bacteria, with an average of  $70 \pm 15\%$  for NCAL and  $72 \pm 25\%$  for CAL,  
429 and was not significantly different between the two experiments. This indicates that most  
430 bacteria in both incubations were particle associated.

431

### 432 3.3 PCA of organic compound composition

433 Results of the principal components analysis (PCA) of the amino acid and pigment  
434 compounds dataset are presented in Tables 3 and 4 and depicted graphically in Fig. 8. One  
435 sample (NCAL AGG, day 10) was removed from the data set because it plotted well outside  
436 the other data. This did not affect the overall pattern of the PCA results, but allowed for  
437 greater separation of the remaining data.

438 The first principal component (PC1) explained 28.7% of the variance in the data, and  
439 the second (PC2) explained 16.3% of the variance. Loadings are listed in Table 3 in order of  
440 their relative contributions to PC1. For PC1, only the loadings of the most useful biomarkers  
441 of degradation will be discussed here. Chlorophyll *a* (Chl *a*) had a relatively large positive  
442 loading on PC1 (0.263), whereas its decomposition products pheophytin (Pptn) and  
443 pheophorbide (Ppb) had highly negative loadings (-0.322 and -0.265, respectively). The non-  
444 protein amino acid  $\beta$ -alanine (BALA), a decomposition indicator (Lee and Cronin, 1982;  
445 Dauwe and Middelburg, 1998), had a negative loading (-0.192). Another non-protein amino  
446 acid commonly used as a decomposition indicator,  $\gamma$ -aminobutyric acid (GABA), was not  
447 detected in any of the samples. Glutamic acid (GLU) and aspartic acid (ASP), two amino

448 acids that tend to be highly concentrated in the cell walls of calcified coccolithophores (Carter  
449 and Mitterer, 1978), differed somewhat in their loadings. GLU had a positive loading (0.202)  
450 whereas ASP had a slightly negative loading (-0.034).

451 None of these six biomarkers had significant loadings on PC2. The hydrophobic  
452 amino acids isoleucine (ILE) and leucine (LEU) had the most positive loadings on PC2 (0.478  
453 and 0.434, respectively), and the hydrophilic amino acids glycine (GLY) and lysine (LYS)  
454 had the most negative loadings (-0.435 and -0.368, respectively).

455 In PCA, samples plot near the variables in which they are enriched (e.g., samples with  
456 positive site scores on PC1 are enriched in variables with positive loadings on that axis). Site  
457 scores are listed in Table 4, grouped according to each sample type. The initial time points  
458 for each sample type (NCAL SUSP day 0, NCAL AGG day 6, CAL SUSP day 0, and CAL  
459 AGG day 0) all had positive site scores on PC1 (1.639, 1.309, 2.061, and 3.759, respectively),  
460 indicating that these samples were enriched in Chl *a*. Site scores for each sample type  
461 progressively decreased over time, suggesting that the samples became increasingly depleted  
462 in Chl *a* and enriched in Pptn, Ppb, and BALA. This is in accordance with the interpretation  
463 that PC1 indicates OM degradation. NCAL samples in general had significantly more  
464 negative PC1 site scores (*t*-test,  $p=0.01$  for comparison of NCAL and CAL SUSP samples,  
465 0.03 for AGG, and 0.0005 for both combined) and also exhibited a significantly greater  
466 decrease over time than CAL samples (F-test,  $p=0.005$  for SUSP, 0.03 for AGG, and 0.002  
467 for both combined). Therefore, NCAL samples were consistently more enriched in Pptn, Ppb,  
468 and BALA.

469 The samples also exhibited significant separation on PC2, with aggregates consistently  
470 having more positive site scores than suspended particles (*t*-test,  $p=0.004$  for comparison of  
471 NCAL AGG and SUSP,  $p=0.008$  for CAL, and  $p=0.0002$  for both combined). Aggregates  
472 were therefore enriched in compounds with positive loadings, such as ILE and LEU, whereas

473 suspended particles were enriched in compounds with negative loadings, such as GLY and  
474 LYS.

475

476

## 477 **4. Discussion**

### 478 4.1 Particulate organic matter degradation

479 Direct comparison between a calcifying and a non calcifying *E. huxleyi* culture during  
480 our incubation experiments revealed that decomposition rates of all total (SUSP+AGG) POM  
481 components investigated were significantly reduced in the presence of biogenic calcite.

482 Overall, the apparent decrease of POC and PN in CAL was very small and the residual

483 percentage of POC and PN left after 30 days of dark incubation was more than twice as high

484 in CAL as in NCAL incubations. Moreover, organic compounds that can be used as

485 biomarkers of decomposition, such as pheopigments and the amino acid  $\beta$ -alanine, became

486 enriched to a higher extent in organic matter of NCAL than CAL. This was shown by PCA

487 analysis of pigments and PAA as well as by the temporal change in the ratio (Pptn+Ppb)/Chl

488 *a* during the experiments. Together, these results strongly suggest that calcified *E. huxleyi*

489 cells were better protected against decomposition than non-calcified cells during our

490 decomposition experiment. Therefore our data support the idea of organic protection through

491 mineral ballast, i.e. settling organic matter in association with calcareous particles may reach

492 the deeper ocean better preserved. The mechanisms that could underlie mineral protection are

493 manifold. Young et al. (1992) suggested that calcification might have evolved as a

494 mechanism to protect the cell's protoplasm against bacterial attack by means of a physical

495 barrier, i.e. the coccosphere. However, thorough investigations that could support this idea are

496 lacking. In an experiment with the dinoflagellate *Scrippsiella trochoidea*, Arnarson and Keil

497 (2005) showed that degradation of organic matter was delayed when clay was added to the

498 incubations. In their experiment some fraction of the mineral protection was attributed to the  
499 sorption of dissolved organic molecules onto the mineral surface. Sorptive preservation of  
500 organic molecules onto clay has been recognized as an important mechanism delaying organic  
501 matter oxidation in sediments (Hedges and Keil 1995). This could be due in part to physical  
502 protection of molecules that are adsorbed within micropores of the mineral surface and  
503 therefore hidden from enzymatic attack (Mayer 1994). Liu and Lee (2007) hypothesize that  
504 the 3-dimensional structure in organic-rich sediments also plays a major role in absorbing  
505 organic compounds, providing a physical protection mechanism for labile organic matter. In  
506 analogy, organic matter and coccoliths may form stable 3D structures that then physically  
507 protect organic matter against degradation.

508         Another mechanism for apparent protection of particulate matter by sorptive  
509 preservation could be that biogenic calcite offers structural support to organic matter that  
510 otherwise would be lost to size fractions  $<0.7 \mu\text{m}$  and hence no longer be detectable as  
511 particulate matter. Because coccoliths provide a structure that can not be broken apart by  
512 bacteria, the association between organic matter and coccoliths, or particulate biogenic  
513 minerals in general, is more likely to keep organic matter in the particulate size fraction  
514 during decomposition. Hence, biogenic calcite would favor the partitioning of organic matter  
515 from the dissolved into the particulate fraction and therewith retain POM during  
516 decomposition. This explanation is supported by our observation that neither bacterial  
517 abundance nor AOU was significantly different between the experiments. Hence, the  
518 microbial degradation of POM and the respiration of organic components might have been  
519 similar, but the loss of POM was retarded in CAL due to the retention of potentially dissolved  
520 organic matter (DOM) on the mineral particles. Because DOM, particles  $<2\mu\text{m}$ , and hydrated  
521 gel particles do not sink gravitationally on their own, they cannot contribute to particle export.

522 Hence, as mentioned earlier biominerals could be ballasting otherwise buoyant fractions of  
523 OM matter into settling processes.

524

525

#### 526 4.2 Differential decomposition of organic matter

527 In both experiments, the total particle volume (PV) decreased significantly with time  
528 by a factor of 5-6. Surprisingly, POC and PN decreased much less than the total PV (Fig. 3).

529 One possible reason for this difference is that POC/N measurements were made on particles  
530  $>0.7 \mu\text{m}$ , while the Coulter Counter measured the volume of particles between 2-60  $\mu\text{m}$ .

531 Therefore, if particles in the range of 0.7-2  $\mu\text{m}$  contained a large proportion of POC (Altabet,  
532 1990), or if highly hydrated gel particles that are not detectable by the Coulter Counter (such  
533 as TEP and Coomassie Blue Stained Particles (CSP)) were abundant, this could explain the  
534 differences we observed. TEP and CSP contain polysaccharides and proteins, respectively,  
535 and are therefore rich in organic carbon. The increase in POC and PN concentration on day 3  
536 of the CAL experiment coincided with an increase in TEP and PAA but not with an increase  
537 in PV. Although TEP could only explain 40% of this POC increase in CAL, it indicates that  
538 formation of gel particles such as TEP and CSP could make a significant contribution to  
539 POM formation.

540 Changes in organic matter during decomposition were revealed by PCA. On the first  
541 principal component axis (PC1), Chl a plotted opposite the decomposition indicators  
542 pheophytin (Pptn), pheophorbide (Ppb), and  $\beta$ -alanine (BALA), suggesting that variance  
543 along PC1 was largely due to biological degradation. These compounds had relatively small  
544 loadings on PC2, indicating that PC1 accounted for most of the compositional variation  
545 resulting from decomposition, whereas PC2 reflected variation due to other processes  
546 (possibly the preferential incorporation of certain amino acids into aggregates, as explained in

547 the next section). Although initial organic compositions of NCAL and CAL samples were  
548 generally similar and plotted near to each other in the PCA, NCAL samples were initially  
549 somewhat more enriched in Pptn, Ppb, and BALA than CAL samples and had more negative  
550 site scores (Fig. 8). This suggests NCAL samples may have undergone some decomposition  
551 prior to initial sampling, during the 5-day aggregation period at the beginning of the  
552 experiment. Over time, the NCAL samples exhibited a greater decrease in Chl *a* and  
553 enrichment with Pptn, Ppb, and BALA than CAL samples, supporting our argument that  
554 NCAL samples decomposed more than CAL samples. Not surprisingly, glutamic acid, which  
555 is often a biomarker for calcareous coccolithophores, plotted near the CAL samples. This  
556 compound also plotted very close to Chl *a*, again suggesting that more calcified samples  
557 tended to be less degraded. However, a similar biomarker for calcareous plankton, aspartic  
558 acid, plotted near the center of the PCA. This amino acid appears to have had equally large  
559 sources in all samples. Glycine can sometimes be enriched in degraded samples (Lee and  
560 Cronin, 1982), although it is also enriched when diatoms are present (Ingalls et al., 2006). Its  
561 enrichment in the NCAL SUSP samples is consistent with those samples being the most  
562 degraded.

563         In both CAL and NCAL experiments the turnover times were lower for TEP than for  
564 POC and lower for PAA than for PN. This may point to a preferential decomposition of  
565 polysaccharides and proteins, but can also be due to diagenesis of organic matter during  
566 decomposition, which may alter compounds to a form where they are no longer detectable by  
567 standard analysis (Lee et al., 2004).

568

#### 569         4.3 Role of TEP and calcite in aggregation

570         During the first 3 days of incubation on the roller table, we observed an increase in  
571 TEP concentration in tanks containing calcifying cells, indicating an enhancement of

572 production and/ or coagulation of dissolved polysaccharides into TEP. Coagulation rates of  
573 DOM into POM might have been higher during the first days of both experiments than in  
574 natural settings due to the high shear initially exerted by the spin-up of the roller tanks. This,  
575 however, does not explain why we observed an increase in TEP formation solely in the  
576 experiment with calcifying algae. Arnarson and Keil (2005) reported an increase of POM  
577 during the initial phase of an experiment when clay was added to a culture of the  
578 dinoflagellate *Scropsiella trochoidea* with no incubation on a roller table. In their experiment,  
579 some fraction of POM formation was attributed to sorption of dissolved organic molecules  
580 onto the mineral surface. Coccoliths of *E. huxleyi* are partly covered by acidic  
581 polysaccharides at the time of their production (de Jong et al. 1976, van Emburg et al. 1986).  
582 Similar to the polysaccharides forming TEP, this coccolith polysaccharide contains ester  
583 sulfate and uronic acid groups that bind  $\text{Ca}^{2+}$  (de Jong et al. 1979) and stain with Alcian Blue  
584 (Engel et al. 2004). To what extent the coccolith polysaccharide cover may enhance the  
585 sorption of DOM, irrespective of dissolved polysaccharides, is unknown. Primary production  
586 as an alternative source for TEP production in CAL seems unlikely since the experiments  
587 were conducted in the dark. We cannot exclude the possibility that calcifying cells during our  
588 experiment produced more dissolved acidic polysaccharides than naked cells and thus had a  
589 higher concentration of TEP precursors initially, consequently leading to more TEP  
590 production during the spin-up of roller tanks. De Jong et al. (1979), however, observed that  
591 calcifying cells produce less dissolved polysaccharides than naked cells. Also, we did not  
592 observe higher TEP formation in CAL cells prior to the experiment, i.e. both incubations had  
593 similar TEP concentration initially. We therefore suggest that coccoliths may act as an  
594 aggregation nucleus for colloidal DOM, such as acidic polysaccharides, leading to the  
595 observed higher increase of TEP and POC production during the first days of the experiment.  
596 This hypothesis is supported by the observation that the fraction of TEP within AGG at the

597 onset of aggregate formation was higher in CAL than in NCAL despite similar initial total  
598 (AGG+SUSP) TEP concentration. Assuming that the coccospheres attracted a higher amount  
599 of acidic polysaccharides than naked cells, these polysaccharides were likely to enhance  
600 stickiness of CAL cells, resulting in faster aggregate formation as demonstrated by video  
601 monitoring (Engel et al., 2007).

602         Alternatively, secondary production of TEP by bacteria could have contributed to total  
603 TEP concentration during the experiment. Using the bacterial production rate of TEP of  
604  $0.11 \pm 0.03 \text{ fg X}_{\text{qev.}} \text{ L}^{-1} \text{ cell}^{-1} \text{ h}^{-1}$  given in Stoderegger and Herndl (1999), we calculated that  
605 bacteria potentially contributed less than 0.5 % to TEP concentration during the first week of  
606 the experiment. Thus they were unlikely to be responsible for the observed doubling in TEP  
607 concentration at day 3. However, due to increasing bacteria abundance and decreasing TEP,  
608 bacterial contribution to TEP may have been as high as 17% at the end of the experiment.

609  
610         The ratio of TEP to POC (mol C: mol C) within CAL aggregates decreased during the  
611 experiment without any detectable influence on aggregate stability. The final TEP:POC ratio  
612 in CAL incubations was very similar to the average TEP:POC ratio within NCAL aggregates,  
613 suggesting that a minimum amount of glue (acidic polysaccharides) might be necessary to  
614 keep particles within an aggregate. Relative to total organic carbon or mass this amount of  
615 TEP was fairly small (i.e. ~4% and 0.01-0.02%, respectively). We did not observe  
616 disintegration of aggregates during the experiment. Longer incubations, however, may reveal  
617 decomposition of the residual TEP fraction in AGG, potentially resulting in aggregate  
618 fragmentation.

619

620         4.4 Aggregate decomposition

621 We observed no decrease in organic matter concentration within aggregates during  
622 either 30-d experiment. Investigating the decomposition of diatom cells within aggregates,  
623 Passow et al. (2003) observed that the amount of cells and biogenic matter did not decrease  
624 within aggregates over a 42-d period. They concluded that degradation of cells within  
625 aggregates was either reduced or balanced by simultaneous aggregation of suspended  
626 particles. During this experiment, the highest amount of organic matter was preserved in  
627 aggregates at a time when changes in total organic matter concentration in the tanks were  
628 negligible (days 15-30). Thus, if decomposition had taken place in aggregates and was  
629 balanced by aggregation from suspended particles, we should have observed a massive  
630 decrease of total organic matter during the second half of our experiment.

631 Bacterial colonization precedes organic matter degradation and enhances aggregate  
632 formation partly because bacteria are often encapsulated by sticky material, or release mucus  
633 substances (Decho, 1990). Thus, one might argue that decomposition of aggregates during  
634 this experiment was slower because they were composed of already partially degraded  
635 material that offered bacteria a poor substrate. Chl *a*: PN ratios, however, were significantly  
636 higher and (P<sub>p<sub>tn</sub></sub> + P<sub>p<sub>b</sub></sub>): Chl *a* ratios significantly lower, for AGG than for SUSP, indicating  
637 the presence of relatively fresh algal cells in AGG. We did not observe a marked difference  
638 in the decomposition of AGG and SUSP over time using PC1 as a degradation index (Dauwe  
639 et al. 1999), despite seeing these differences in pheopigment/ chl *a* ratios. However, PC1  
640 does not appear to exclusively indicate degradation, since compounds such as phenylalanine  
641 (PHE), valine (VAL), alanine (ALA), and methionine (MET) that do not necessarily reflect  
642 degradation had large loadings on this axis and may have influenced separation of the data.  
643 AGG and SUSP samples for both cell types were well separated on PC2, indicating that these  
644 samples had compositional differences resulting from processes other than decomposition.  
645 This is extremely interesting, since these fractions were originally derived from the same

646 cultures, and should theoretically have the same composition. Possibly, certain compounds  
647 are preferentially incorporated into aggregates as they form from colloidal or dissolved  
648 organic matter. Differences in hydrophobicity may control this preferential incorporation, as  
649 suggested by the fact that AGG samples plotted near the hydrophobic amino acids leucine and  
650 isoleucine, whereas the SUSP samples plotted near the more hydrophilic amino acids glycine  
651 and lysine. Aggregation and disaggregation processes may therefore change the composition  
652 of particulate organic matter (POM) as it sinks through the water column. We can only  
653 speculate about the mechanisms that could be responsible for reduced decomposition in  
654 aggregates. Compaction of particles within the aggregate could provide a physical barrier if it  
655 resulted in pore sizes too small to allow bacterial attack. At small scales (interstitial pores  
656 about 0.1 - 10 nm in diameter), aggregation may place a physical barrier between organic  
657 substrates and decomposing organisms or their extracellular enzymes (Baldock and  
658 Skjemstad, 2000). Previous studies on soil aggregates have found that bacteria can only exist  
659 within aggregates when the interstitial pore spaces are at least three times their own diameter  
660 (Oades, 1988; Baldock and Skjemstad, 2000). However, it is not yet known whether the  
661 physical exclusion of bacteria or exo-enzymes from aggregates occurs in the water column.  
662 Although we observed bacteria in the AGG fraction, it is not possible to determine whether  
663 these bacteria were actually within the aggregates or merely on their surfaces (counting  
664 bacteria requires aggregate disruption, so the original location of bacteria cannot be  
665 determined). Bacteria abundances were higher by two orders of magnitude in AGG than in  
666 SUSP (data not shown) and comparable to abundances observed previously on marine snow  
667 (Smith et al., 1992). High bacterial densities were previously thought to lead to rapid  
668 dissolution of POM in aggregates during short-term incubations (Smith et al., 1992), or during  
669 the initial phase of long-term incubations (Grossart and Ploug, 2001). During this  
670 experiment, however, high bacterial densities on aggregates did not cause significant

671 solubilization of aggregated organic matter. Again, bacteria may have only been present on  
672 the surface, and physically excluded from the interior of the aggregates. Also, Grossart and  
673 Ploug (2001) suggested that the decrease they observed in bacterial activity on aggregates  
674 with time was due to increasing grazing pressure of attached protozoa. We did not look at  
675 heterotrophic flagellates during this experiment. However, since we observed no significant  
676 decrease in the amount of POM and bacteria in aggregates, total grazing and subsequent  
677 respiratory losses of carbon must have been small.

678         Because our experiment was limited to a 30-d period, we cannot exclude the  
679 possibility that aggregate decomposition occurs on longer time scales. How effectively  
680 aggregates will export organic matter to the deep ocean might therefore depend primarily on  
681 the settling velocity, i.e., whether an aggregate reaches the deep sea within weeks rather than  
682 months. Determination of aggregate formation, size and settling velocities during this  
683 experiment revealed that aggregates in CAL formed earlier and sank faster than in NCAL  
684 (Engel et al., 2007).

685

686

## 687         **5. Conclusion**

688         This study showed that the decomposition rate of most particulate organic components  
689 is slowed down in calcifying cells of the species *Emilinia huxleyi* compared to non-calcifying  
690 cells. Calcifying and non-calcifying cells both formed macroscopic aggregates whose  
691 chemical compositions were different from suspended particulate matter in the surrounding  
692 seawater. No decomposition of aggregates was observed within the 30 day period of both  
693 experiments. Our results suggest that biogenic calcite plays an important role in the  
694 preservation of particulate organic matter in seawater.

695

696

697

698

**Acknowledgements**

699

This work was supported by NSF grants OCE 01-36370 and 04-24845 (MedFlux), and

700

by the Helmholtz Association (HZ-NG-102). The first author was supported by the Max

701

Kade Foundation of New York. We thank Markus Schartau for fruitful discussion on PCA.

702

This is publication AWI n-17023, MSRC 1356, and MedFlux 17.

703

704 **References**

- 705 Alldredge, A. L., C. Gottschalk, C., 1988. In situ settling behavior of marine snow.  
706 *Limnology and Oceanography* 33, 339-351.
- 707 Altabet, M. A., 1990. Organic C, N, and stable isotopic composition of particulate matter  
708 collected on glass-fiber and aluminum oxide filters. *Limnology and Oceanography* 35,  
709 902-909.
- 710 Armstrong, R. A., Lee, C., Hedges, J.I., Honjo, S., Wakeham, S.G., 2002. A new,  
711 mechanistic model for organic carbon fluxes in the ocean based on the quantitative  
712 association of POC with ballast minerals. *Deep-Sea Research II* 49, 219-236.
- 713 Arnarson, T. S., Keil, R.G., 2001. Organic-mineral interactions in marine sediments studied  
714 using density fractionation and X-ray photoelectron spectroscopy. *Organic Geochemistry*  
715 32, 1401-1415.
- 716 Arnarson, T. S., Keil, R.G., 2005. Influence of organic-mineral aggregates on microbial  
717 degradation of the dinoflagellate *Scrippsiella trochoidea*. *Geochimica. et Cosmochimica*  
718 *Acta* 69, 2111–2117.
- 719 Baldock, J. A., Skjemstad, J.O., 2000. Role of the soil matrix and minerals in protecting  
720 natural organic materials against biological attack. *Organic Geochemistry* 31, 697-710.
- 721 Bidigare, R. R., Kennicutt, M.C., Brooks, J.M., 1985. Rapid determination of chlorophylls  
722 and their degradation products by high-performance liquid chromatography. *Limnology*  
723 *and Oceanography* 30, 432-435. Carter, P. W., Mitterer, R.M., 1978. Amino acid  
724 composition of organic matter associated with carbonate and non-carbonate sediments.  
725 *Geochimica et Cosmochimica Acta* 42, 1231-1238.
- 726 Dauwe, B., Middelburg, J.J., 1998. Amino acids and hexosamines as indicators of organic  
727 matter degradation state in North Sea sediments. *Limnology and Oceanography* 43, 782-  
728 798.

- 729 Dauwe, B., Middelburg, J.J., Herman, P.M.J., Heip, C.H.R., 1999. Linking diagenetic  
730 alteration of amino acids and bulk organic matter reactivity. *Limnology and Oceanography*  
731 44, 1809-1814.
- 732 Decho, A. W., 1990. Microbial exopolymer secretions in ocean environments: Their role(s) in  
733 food webs and marine processes. *Oceanography and Marine Biology. An Annual Review*  
734 28, 73-153.
- 735 de Jong, E. W., Bosch, L., Westbroek, P., 1976. Isolation and characterization of a Ca<sup>2+</sup>-  
736 binding polysaccharide associated with coccoliths of *Emiliana huxleyi* (Lohmann)  
737 Kamptner. *European Journal of Biochemistry* 70, 611-621.
- 738 de Jong, E. W., van Rens, L., Westbroek, P., Bosch, L., 1979. Biocalcification by the marine  
739 alga *Emiliana huxleyi* (Lohmann) Kamptner. *European Journal of Biochemistry* 99, 559-  
740 567.
- 741 Delille B., Harlay, J., Zondervan, I., Jacquet, S., Chou, L., Wollast, R., Bellerby, R.G.J.,  
742 Frankignoulle, M., Borges, A.V., Riebesell, U., Gattuso, J.-P., 2005. Response of primary  
743 production and calcification to changes of pCO<sub>2</sub> during experimental blooms of the  
744 coccolithophorid *Emiliana huxleyi*. *Global Biogeochemical Cycles* 19 (GB2023),  
745 doi:10.1029/2004GB002318.
- 746 Duchaufour, P., 1976. Dynamics of organic matter in soils of temperate regions: its action on  
747 pedogenesis. *Geoderma* 15, 31-40.
- 748 Engel, A., Delille, B., Jacquet, S., Riebesell, U., Rochelle-Newall, E., Terbrüggen, A.,  
749 Zondervan, I., 2004. TEP and DOC production by *Emiliana huxleyi* exposed to  
750 different CO<sub>2</sub> concentrations: A mesocosms experiment. *Aquatic Microbial Ecology*  
751 34, 93-104.

- 752 Engel, A., Szlosek, J., Abramson, L., Liu, Z., Lee, C., 2008. Investigating the effect of  
753 ballasting by  $\text{CaCO}_3$  in *Emiliania huxleyi*: I. Formation, settling velocities and  
754 physical properties of aggregates. Deep-Sea Research II, submitted.
- 755 Ferguson, R. I., Buckley, E. N., Palumbo, A. V., 1984. Response of marine bacterioplankton  
756 to differential filtration and confinement. Applied Environmental Microbiology 47,  
757 49-55.
- 758 Fowler, S.W., Knauer, G. A., 1986. Role of large particles in the transport of elements and  
759 organic compounds through the oceanic water column. Progress in Oceanography 16,  
760 147-194.
- 761 François, R., Honjo, S., Krishfield, R., Manganini, S., 2002. Factors controlling the flux of  
762 organic carbon to the bathypelagic zone of the ocean. Global Biogeochemical Cycles  
763 16, 1087, doi: 10.1029/2001GB001722.
- 764 Grossart, H.-P., Ploug, H., 2001. Microbial degradation of organic carbon and nitrogen on  
765 diatom aggregates. Limnology and Oceanography 46, 267-277.
- 766 Guillard, R. R. L., 1975. Culture of phytoplankton for feeding marine invertebrates, p. 26-60.  
767 In W. L. Smith and M. H. Chanley [eds.], Culture of Marine Invertebrate Animals. Plenum  
768 Press, New York.
- 769 Hedges, J. I., Keil, R.G., 1995. Sedimentary organic matter preservation: An assessment and  
770 speculative synthesis. Marine Chemistry 49, 81-115.
- 771 Hobbie, J. E., Daley, R.J., Jasper, S., 1977. Use of nuclepore filters for counting bacteria by  
772 fluorescence microscopy. Applied Environmental Microbiology 33, 1225-1228.
- 773 Ingalls, A. E., Liu, Z., Lee, C., 2006. Seasonal trends in pigment and amino acid compositions  
774 of sinking particles in biogenic  $\text{CaCO}_3$  and  $\text{SiO}_2$  dominated regions of the Pacific sector of  
775 the Southern Ocean along  $170^\circ\text{W}$ . Deep-Sea Research I 53, 836-659.
- 776 Ittekkot, V., Haake, B., 1990. The terrestrial link in the removal of organic carbon. In:

- 777 Ittekkpot, V., Kempe, S., Michaelis, M., Spitzzy, A. (Eds.) Facets of Modern  
778 Biogeochemistry. Springer, Berlin, pp. 319-325.
- 779 Klaas, C., Archer, D., 2002. Association of sinking organic matter with various types of  
780 mineral ballast in the deep sea: Implications for the rain ratio. *Global Biochemical Cycles*  
781 16, 1116. [doi: 10.1029/2001GB001765]
- 782 Lee, C., Cronin, C., 1982. The vertical flux of particulate nitrogen in the sea: Decomposition  
783 of amino acids in the Peru upwelling area and the equatorial Atlantic. *Journal of Marine*  
784 *Research* 40, 227-251.
- 785 Lee, C., Cronin, C., 1984. Particulate amino acids in the sea: Effects of primary productivity  
786 and biological decomposition. *Journal of Marine Research* 42, 1075-1097.
- 787 Lee, C., Wakeham, S.G., Hedges, J.I., 2000. Composition and flux of particulate amino acids  
788 and chloropigments in equatorial Pacific seawater and sediments. *Deep-Sea Research I* 47,  
789 1535-1568.
- 790 Lee, C., Wakeham, S.G., Arnosti, C., 2004. Particulate organic matter in the sea: The  
791 composition conundrum. *Ambio* 33, 565-575.
- 792 Lewis, E., Wallace, D.W.R., 1998. Program developed for CO<sub>2</sub> System Calculations.  
793 ORNL/CDIAC-105. Carbon Dioxide Information Analysis Center, Oak Ridge National  
794 Laboratory, U. S. Department of Energy, Oak Ridge, Tennessee.
- 795 Liu, Z., Lee, C., 2007. The role of organic matter in the sorption capacity of marine  
796 sediments. *Marine Chemistry* 105, 240-257
- 797 Lindroth, P., Mopper, K. 1979. High performance liquid chromatographic determination of  
798 subpicomole amounts of amino acids by precolumn fluorescence derivitaziation with *o*-  
799 phthdialdehde. *Analytical Chemistry* 51, 1667-1674.

- 800 Mantoura, R. F. C., Llewellyn, C.A., 1983. The rapid determination of algal chlorophyll and  
801 carotenoid pigments and their breakdown in natural waters by reverse-phase high-  
802 performance liquid chromatography. *Analytica Chimica Acta* 151, 297-314.
- 803 Mantoura, R.F.C., Llewellyn, C. A.. 1984. Trace enrichment of marine algal pigments for use  
804 with HPLC-diode array spectroscopy. *Journal of High Resolution Gas Chromatography*  
805 *and Chromatography Communications* 7, 632- 635. Martin, J. H., Knauer, G.A., Karl,  
806 D.M., Broenkow, W.W., 1987. VERTEX: Carbon cycling in the northeast Pacific. *Deep-*  
807 *Sea Research I* 34, 267-285.
- 808 Mayer, L. M., 2004. The inertness of being organic. *Marine Chemistry* 92, 135-140.
- 809 McCave, I.N., 1975. Vertical flux of particles in the ocean. *Deep-Sea Research* 22, 491–502.
- 810 Mehrbach, C., Culberson, C.H., Hawley, J.E., Pytkowicz, R.M., 1973. Measurement of the  
811 apparent dissociation constants of carbonic acid in seawater at atmospheric pressure.  
812 *Limnology and Oceanography* 18, 897-907.
- 813 Milliman, J. D., 1993. Production and accumulation of calcium carbonate in the ocean:  
814 Budget of a nonsteady state. *Global Biogeochemical Cycles* 7, 927-957. [doi:  
815 10.1029/93GB02524]
- 816 Oades, J. M., 1988. The retention of organic matter in soils. *Biogeochemistry* 5, 35-70.
- 817 Parsons, T., Maita, Y., Lalli, C.M., 1984. A manual of chemical and biological methods for  
818 seawater analysis. Pergamon.
- 819 Peng. T.-H., Takahashi, T., Broecker, W.S., Olafsson, J., 1987. Seasonal variability of carbon  
820 dioxide, nutrients and oxygen in the northern North Atlantic surface water. *Observations*  
821 *and a model. Tellus.* 39B, 439-458.
- 822 Passow, U., Alldredge, A.L., 1995. A dye-binding assay for the spectrophotometric  
823 measurement of transparent exopolymer particles (TEP). *Limnology and Oceanography*  
824 40, 1326-1335.

- 825 Passow, U., Engel, A., Ploug, H., 2003. The role of aggregation for the dissolution of diatom  
826 frustules. *FEMS Microbiology Ecology* 46, 247-255.
- 827 Redfield, A. C., Ketchum, B.H., Richards, F.A., 1963. The influence of organisms on the  
828 composition of seawater, p. 26-79. *In* M.N. Hill [ed.], *The sea*, Vol. 2. Wiley Interscience,  
829 New York.
- 830 Riebesell, U., Wolf-Gladrow, D. A., Smetacek, V., 1993. Carbon dioxide limitation of marine  
831 phytoplankton growth rates. *Nature* 361, 249-251.
- 832 Sachs, L., 1974. *Angewandte Statistik*. Springer Verlag Berlin Heidelberg New York.
- 833 Shanks, A. L., Edmondson, E.W., 1989. Laboratory-made artificial marine snow: A biological  
834 model of the real thing. *Marine Biology* 101, 463-470.
- 835 Sheridan, C. C., Lee, C., Wakeham, S.G., J. K. B. Bishop, J.K.B., 2002. Suspended particle  
836 organic composition and cycling in surface and midwaters of the equatorial Pacific Ocean.  
837 *Deep-Sea Research I* 49, 1983-2008.
- 838 Smayda, T.J., 1970. Normal and accelerated sinking of phytoplankton in the sea.  
839 *Oceanography and Marine Biology* 8, 353-414.
- 840 Smith, D. C., Simon, M., Alldredge, A.L., F. Azam, F., 1992. Intense hydrolytic enzyme  
841 activity on marine aggregates and implications for rapid particle dissolution. *Nature* 359,  
842 139-142.
- 843 Stoderegger, K. E., Herndl, G.J., 1999. Production of exopolymer particles by marine  
844 bacterioplankton under contrasting turbulence conditions. *Marine Ecology Progress Series*  
845 189, 9-16.
- 846 Suess, E., 1973. Interaction of organic compounds with calcium-carbonate. Organo-carbonate  
847 association in recent sediments. *Geochimica et Cosmochimica Acta* 37, 2435-.

- 848 Sun, M., Aller, R.C., Lee, c.. 1991. Early diagenesis of chlorophyll-a in Long Island Sound  
849 sediments: A measure of carbon flux and particle reworking. *Journal of Marine Research*  
850 49, 1-23.
- 851 Suzuki, M. T., Sherr, E.B., Sherr, B.F., 1993. DAPI direct counting underestimates bacterial  
852 abundances and average cell size compared to AO direct counting. *Limnology and*  
853 *Oceanography* 38, 1566-1570.
- 854 Turley, C. M., Hughes, D.J., 1994. The effect of storage temperature on bacterial cell loss due  
855 in preserved seawater samples. *Journal of the Marine Biological Association UK* 74, 259-  
856 262.
- 857 Van Emburg, P. R., de Jong, E.W., Daems, W.T.H., 1986. Immunochemical localization of a  
858 polysaccharide from biomineral structures (coccoliths) of *Emiliania huxleyi*. *Journal of*  
859 *Ultrastructure and Molecular Structure Research* 94, 259-264.
- 860 Young, J.R., Didymus, J.M., Bown, P.R., Prins, B., Mann, S., 1992. Crystal assembly and  
861 phylogenetic evolution in heterococcoliths. *Nature* 356, 516–518.
- 862 Zobel, C. E., Anderson, D.Q., 1932. Observations on the multiplication of bacteria in different  
863 volumes of stored seawater and the influence of oxygen tension and solid surfaces.  
864 *Biological Bulletin* 71, 341-342.  
865

Table 1. Abbreviations

ALA	alanine	AO	Acridine Orange
ARG	arginine	ASP	aspartic acid
BALA	$\beta$ -alanine	CAL	calcifying <i>E. huxleyi</i> cells
Chl	chlorophyll	Corg	organic carbon
CSP	Coomassie Blue stained particles	DAPI	
ESD	equivalent spherical diameter	GABA	$\gamma$ -aminobutyric acid
GLU	glutamic acid	GLY	glycine
HIS	histidine	HPLC	high-performance liquid chromatography
ILE	isoleucine	LEU	leucine
LYS	lysine	MET	methionine
Min	mineral	NCAL	non-calcifying <i>E. huxleyi</i> cells
OM	organic matter	PAA	total particulate amino acids
PCA	principal components analysis	PHE	phenylalanine
PIC	particulate inorganic carbon	PN	particulate nitrogen
POC	particulate organic carbon	POM	particulate organic matter
Pptn	pheophytin	Ppb	pheophorbide
PV	particle volume	SER	serine
SUSP	particles in surrounding seawater	TEP	transparent exopolymer particles
THR	threonine	TPC	total particulate carbon
TPN	total particulate nitrogen	TYR	tyrosine
VAL	valine	Xeq	xanthum gum equivalent

868

869 Table 2: Regression statistics for the first-order exponential decay of total organic matter

870 components over time. The decay rate constant ( $k$ ) was always calculated using the highest

871 concentration as initial value. Significance level of difference between NCAL and

872 CAL:\*\*&lt;0.001, \*&lt;0.01.

<i>time</i> ( <i>t</i> , days)	variable (y)	decay rate ( $k$ , d <sup>-1</sup> )	standard deviation of ( $k$ )	correlation coefficient ( $r^2$ )	number of observations ( $n$ )
<i>Calcified E. huxleyi</i> (CAL)					
3-30	POC	0.012**	0.0046	0.997	6
3-30	PN	0.012**	0.0057	0.999	6
3-30	TEP	0.040*	0.0125	0.985	6
3-30	PAA	0.037*	0.0081	0.993	6
1-30	TPV	0.043**	0.0114	0.988	7
1-30	Chl <i>a</i>	0.060**	0.0043	0.998	6
<i>Non-calcified E. huxleyi</i> (NCAL)					
3-30	POC	0.016	0.0161	0.997	6
3-30	PN	0.039	0.0148	0.979	6
3-30	TEP	0.058	0.0164	0.982	6
3-30	PAA	0.027	0.0089	0.990	6
1-30	TPV	0.129	0.021	0.992	7
1-30	Chl <i>a</i>	0.130	0.030	0.967	7

873

874

875

876

877 Table 3. Variable loadings in the principal components analysis (PCA) in order of  
 878 their relative contributions to PC1. Bold fonts indicate key indicators of freshness or  
 879 degradation.

880

Variable	Loadings	
	PC1	PC2
PHE	0.304	-0.033
VAL	0.299	0.067
<b>Chl a</b>	<b>0.263</b>	<b>0.075</b>
HIS	0.246	0.002
SER	0.244	-0.150
<b>GLU</b>	<b>0.202</b>	<b>0.005</b>
ARG	0.149	0.266
LYS	0.107	-0.368
ILE	0.102	0.478
<b>ASP</b>	<b>-0.034</b>	<b>0.076</b>
LEU	-0.082	0.434
THR	-0.115	0.262
GLY	-0.183	-0.435
<b>BALA</b>	<b>-0.192</b>	<b>0.113</b>
TYR	-0.263	-0.107
<b>Ppb</b>	<b>-0.265</b>	<b>-0.067</b>
MET	-0.315	0.222
<b>Pptn</b>	<b>-0.322</b>	<b>0.042</b>
ALA	-0.332	-0.012

881

882

883

884

885

886

887

888

889

890

891

892

Table 4. Sample site scores in the principal component analysis (PCA).

Object	Scores	
	PC1	PC2
<b>NCAL-SUSP</b>		
Day 0	1.639	-1.684
Day 3	0.068	-1.535
Day 6	-0.537	0.182
Day 10	-1.558	-0.787
Day 16	-2.651	-2.157
Day 23	-4.539	0.026
Day 30	-2.168	-0.566
<b>NCAL-AGG</b>		
Day 6	1.309	0.920
Day 16	-4.490	0.800
Day 23	-3.411	2.563
Day 30	-4.364	0.945
<b>CAL-SUSP</b>		
Day 0	2.061	-1.861
Day 3	1.685	-0.847
Day 6	0.774	-2.200
Day 10	0.716	-1.914
Day 16	1.222	-1.195
Day 23	0.362	-1.120
Day 30	1.478	-0.318
<b>CAL-AGG</b>		
Day 0	3.759	1.730
Day 3	2.046	1.639
Day 6	1.437	5.761
Day 10	2.147	0.700
Day 16	1.692	0.412
Day 23	1.425	0.365
Day 30	-0.102	0.141

893

894

895

896

897

898

899 **Figure Legends**

900 Figure 1: Schematic presentation of the experimental set-up and sampling. Two  
901 identical experiments were conducted in the dark. Calcifying (CAL) and non-calcifying  
902 (NCAL) *E. huxleyi* cells were grown in batch cultures and incubated in 8 tanks on a rolling  
903 table to promote aggregation (I-II). After 5d about 3/4 of the tank water was replaced by  
904 filtered seawater to incubate aggregates in a more dilute media (III-IV). The tanks were  
905 placed again on the roller table to simulate continuous sinking of formed aggregates for 30  
906 more days (V). One tank was harvested at each sampling date and aggregates (AGG) were  
907 removed from the surrounding seawater by a syringe (VI). AGG and suspended particles  
908 without aggregates (SUSP) were then analyzed separately.

909

910

911 Figure 2: Changes in the total volume of solid particles  $> 2\mu\text{m}$  as determined by  
912 Coulter counter during the two 30-d incubations. Symbols: open rectangles, total particle  
913 volume in NCAL incubations; solid rectangles, total particle volume in CAL incubations.  
914 Also shown are the changes in particulate volume of aggregates alone. Symbols: open  
915 triangles, particle volume in aggregates in NCAL incubations; solid triangles, particle volume  
916 in aggregates in CAL incubations.

917

918 Figure 3 a, b: Decrease of total particulate organic carbon (POC, a) and total  
919 particulate nitrogen (PN, b) concentration during the experiments with a calcifying (solid line)  
920 and a non-calcifying (dotted line) *E. huxleyi* strain. Also shown are the changes in POC and  
921 PON concentration within aggregates. Symbols as in Fig. 2.

922

923 Figure 4: Total and AGG Chlorophyll *a* (Chl *a*) concentration during the experiment  
924 in NCAL and CAL. Symbols as in Fig. 2.

925

926 Figure 5: Total transparent exopolymer particles (TEP) concentration, expressed as  
927 carbon contained in TEP, during the experiment as determined with the colorimetric method.  
928 Symbols as in Fig. 2.

929

930 Figure 6: Total particulate amino acid (PAA) concentration during the decomposition  
931 experiments. Symbols as in Fig. 2.

932

933 Figure 7: Total bacteria abundances during the decomposition experiments,  
934 determined microscopically after staining with Acridine Orange. Open rectangles: NCAL,  
935 solid rectangles: CAL. Bacteria concentration on day 16 were  $88 \pm 4.1 \times 10^5$  for NCAL and  
936  $243 \pm 3.9 \times 10^5$  and were not included in the figure to allow easier presentation of the data.

937

938 Figure 8: Graphical representation of the principal component analysis. Bold  
939 crosshairs in the center of each plot represents 'mean' sample. Top panel: amino acid loadings  
940 (key indicators of freshness/ degradation shown in larger font). Bottom: sample site scores.  
941 Open triangles: NCAL-AGG, solid triangles: CAL-AGG, open diamonds: NCAL SUSP, solid  
942 diamonds: CAL-SUSP. Numbers represent days on which samples were collected.

943

944

945

946

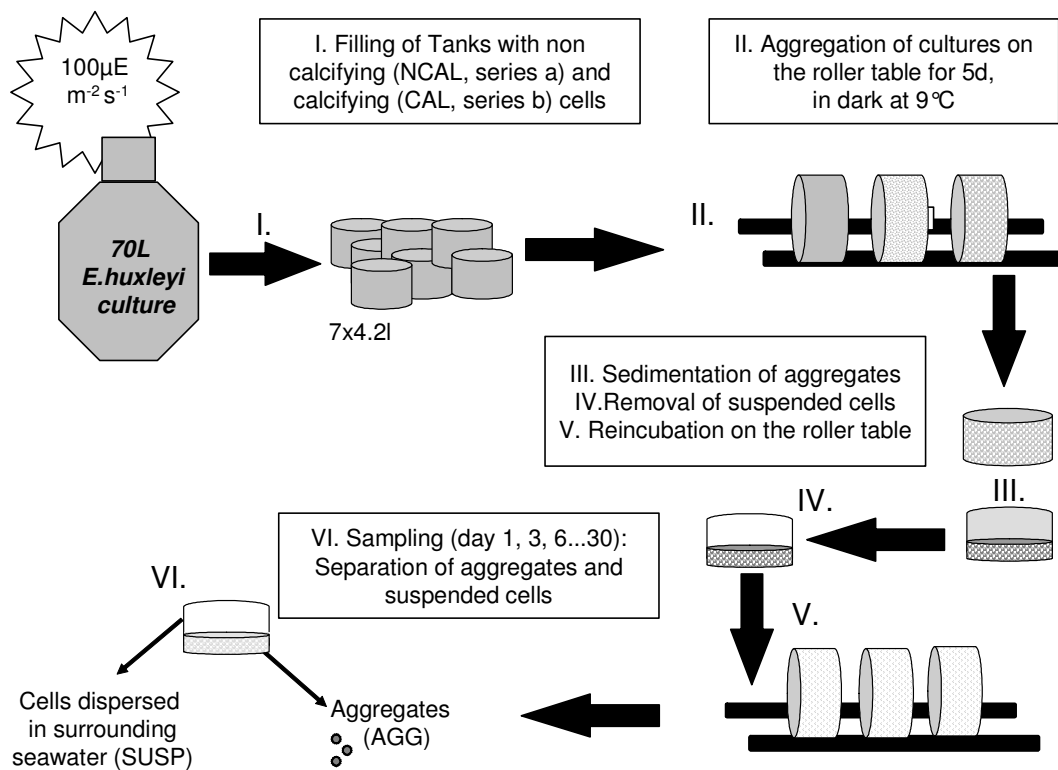
947

948

949

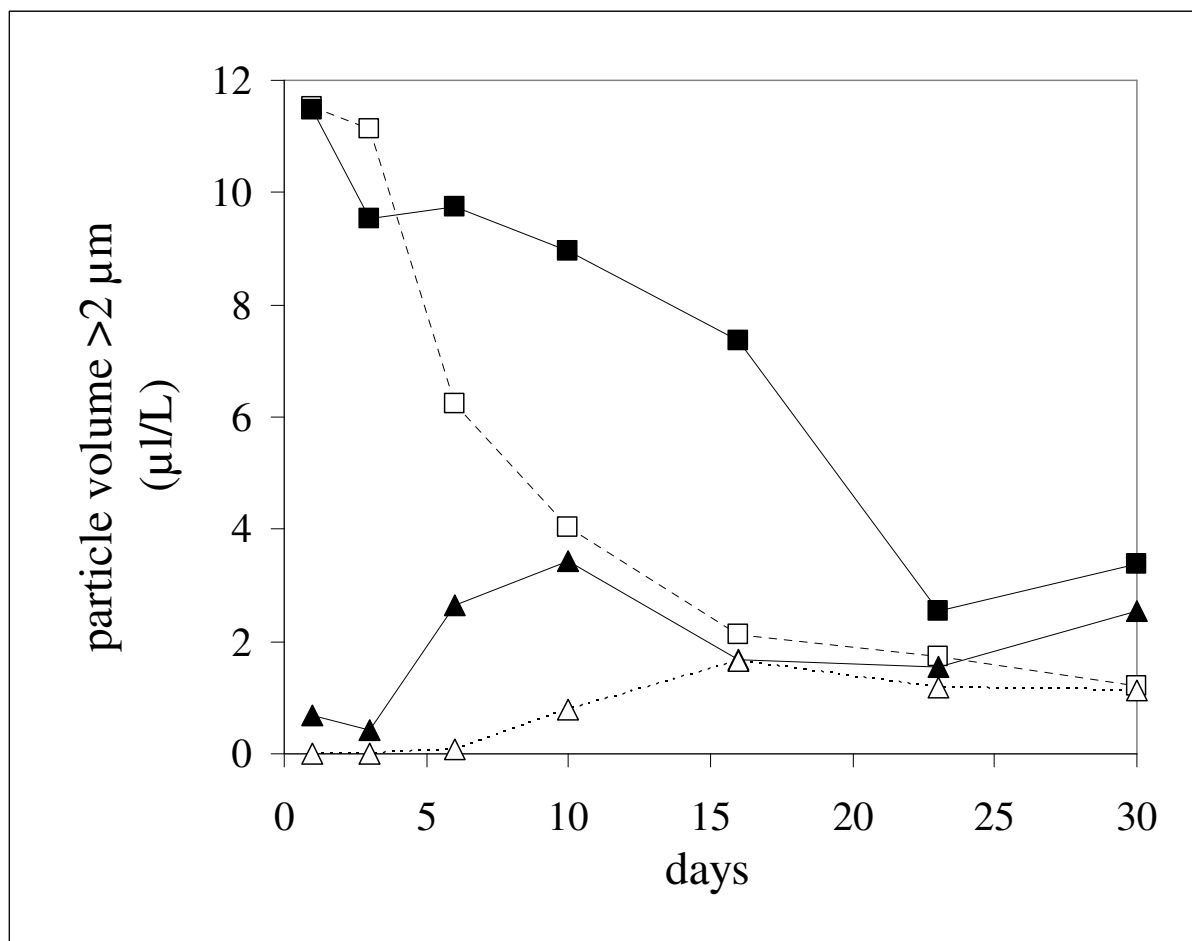
950

951  
952



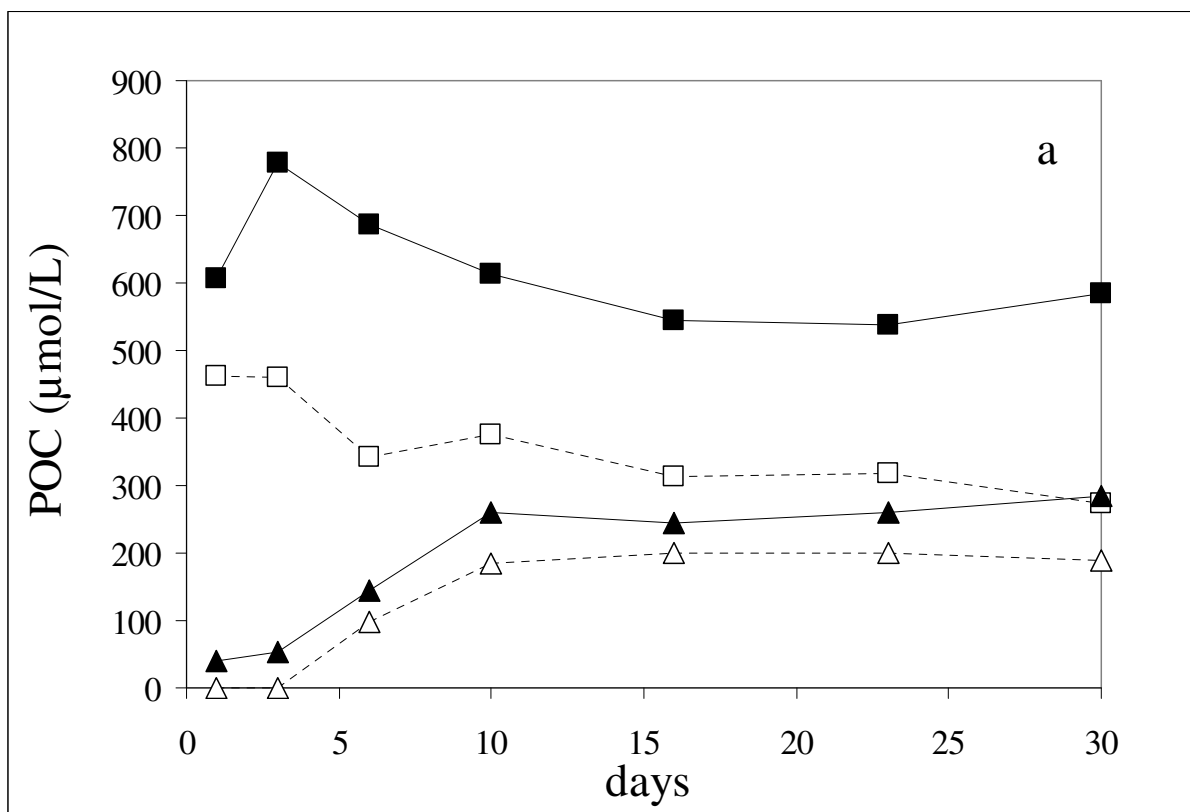
953  
954  
955  
956  
957  
958  
959  
960

Engel et al., Figure 1

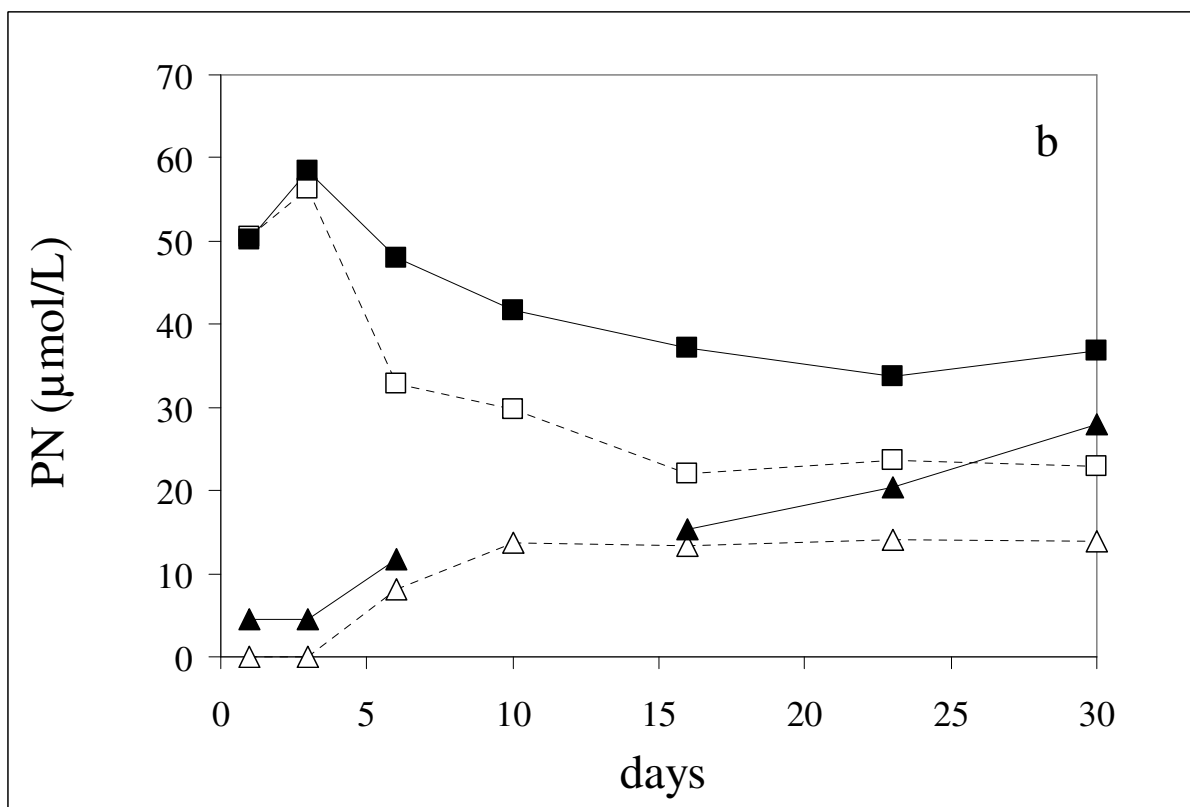


961  
962  
963  
964  
965

Engel et al., Figure 2



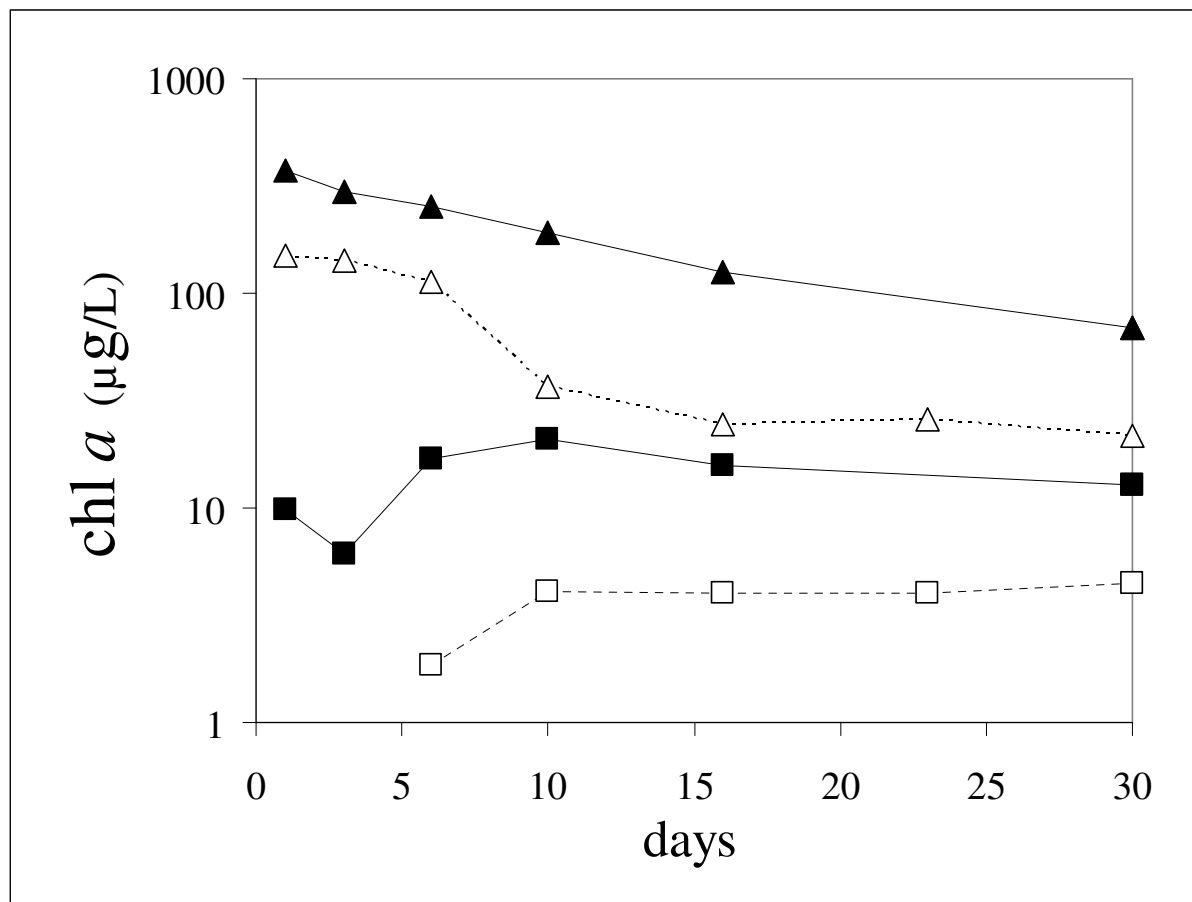
966



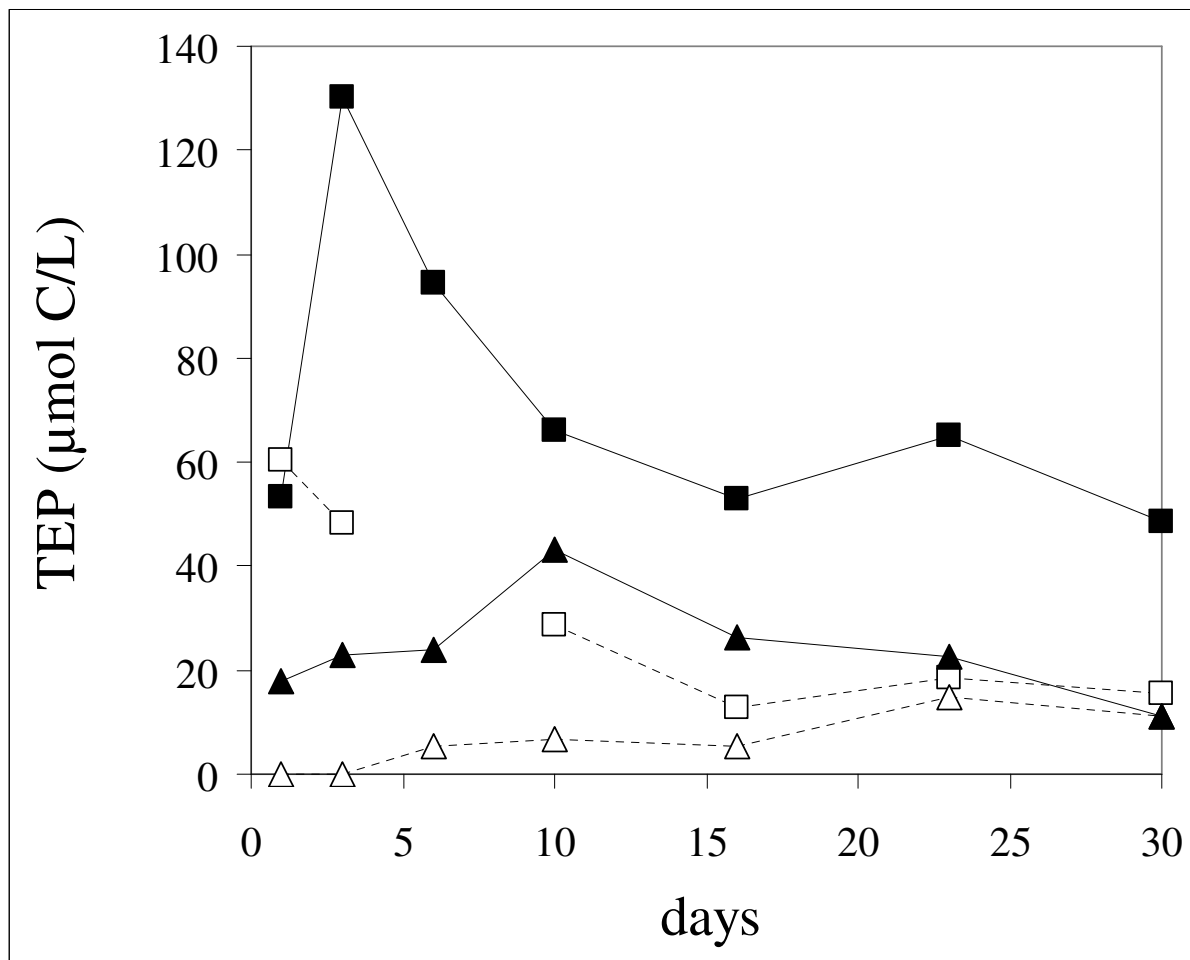
967  
 968  
 969  
 970  
 971

Engel et al., Figure 3a, b

972

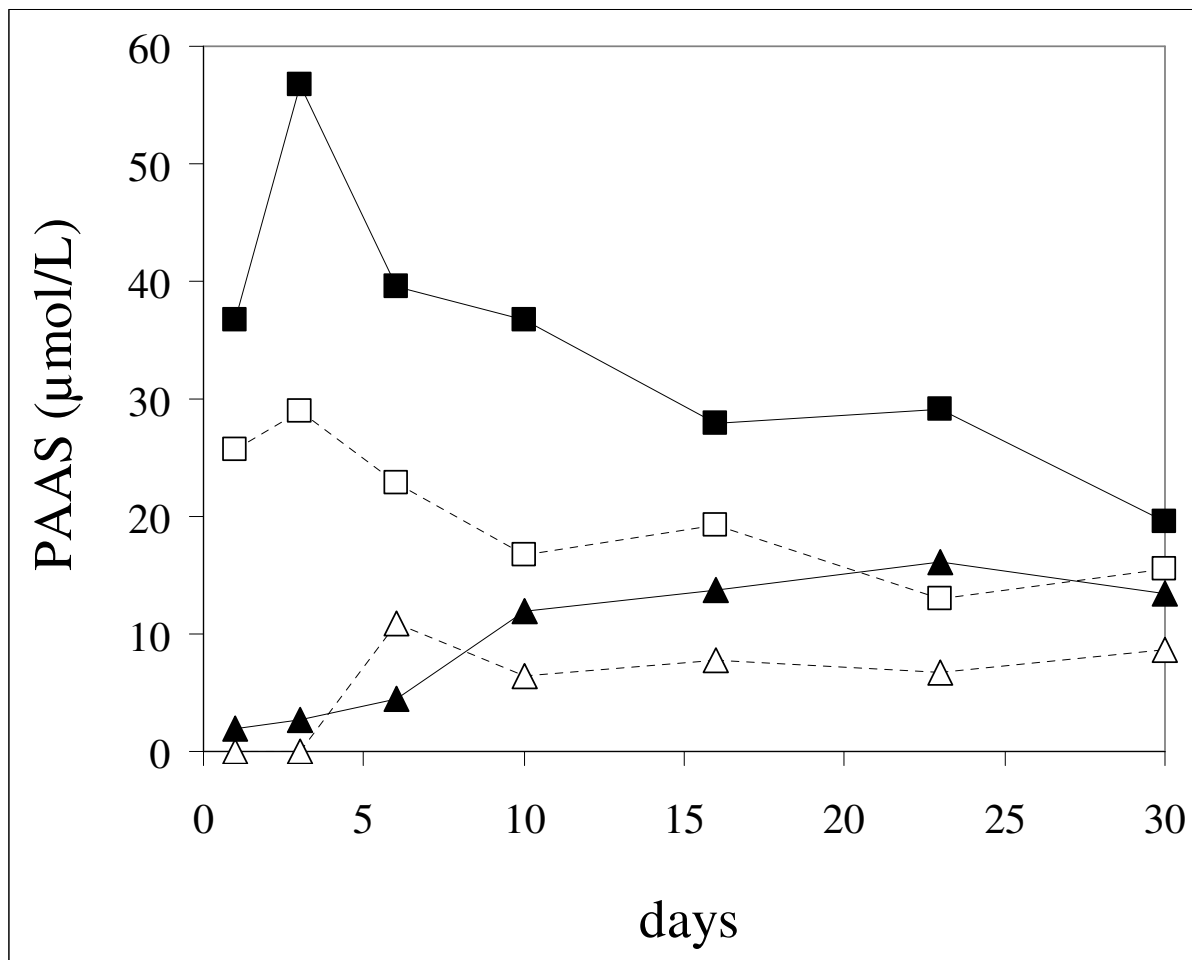
973  
974  
975  
976

Engel et al., Figure 4



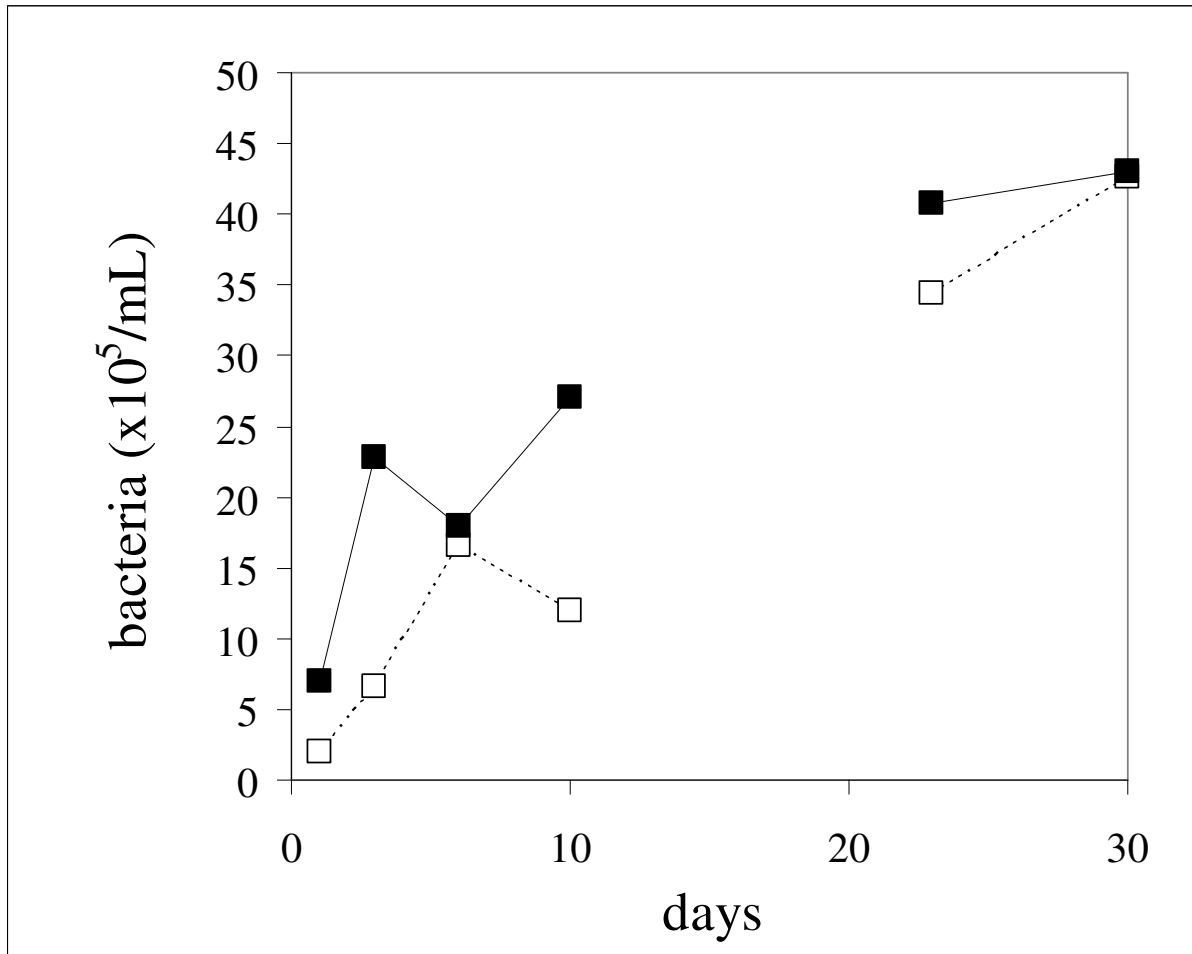
977  
978  
979  
980  
981  
982  
983  
984  
985

Engel et al., Figure 5



986  
987  
988  
989  
990  
991  
992  
993  
994  
995  
996  
997  
998

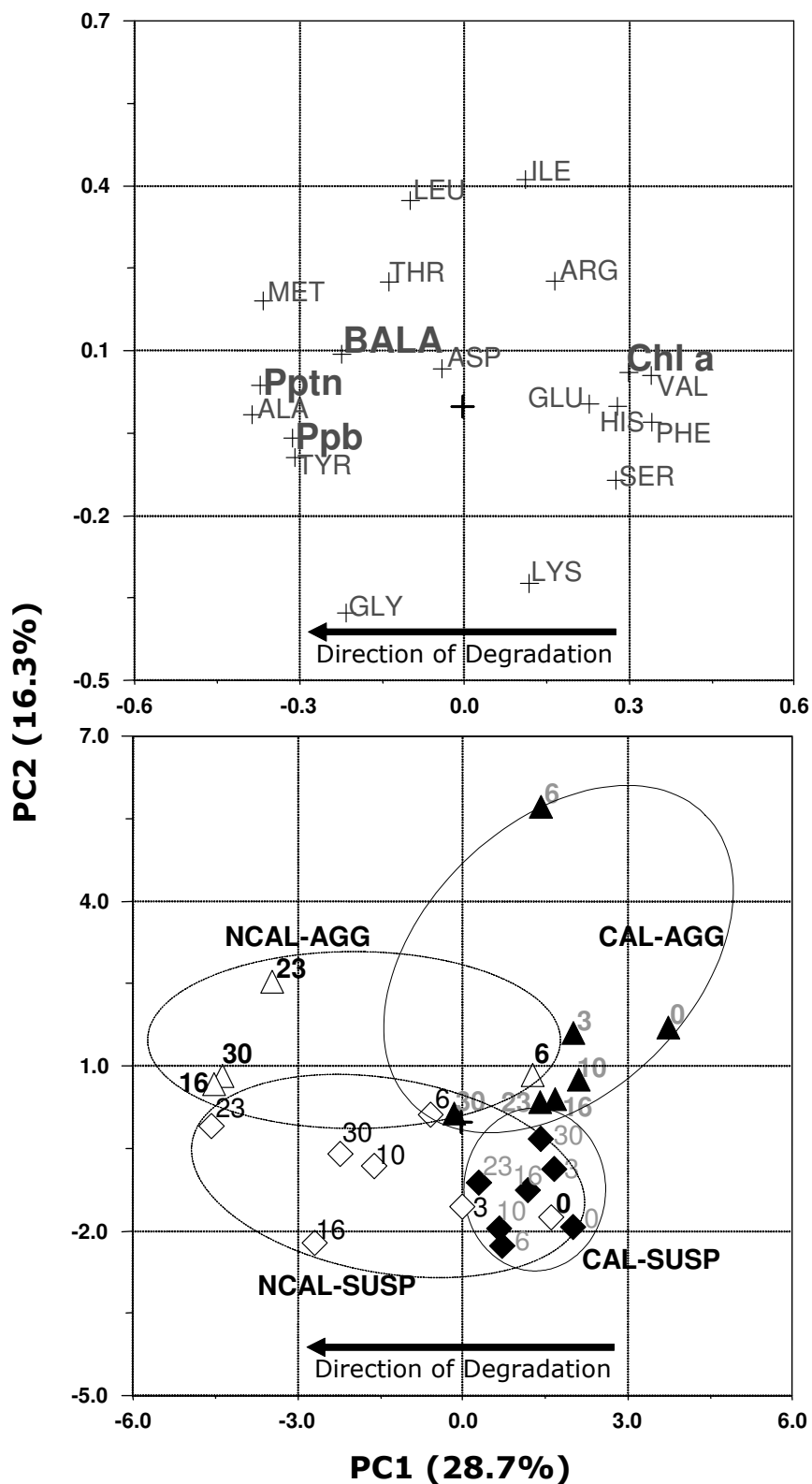
Engel et al., Figure 6



Engel et al., Figure 7

999  
1000  
1001  
1002  
1003  
1004  
1005  
1006  
1007  
1008  
1009  
1010  
1011  
1012  
1013  
1014  
1015  
1016  
1017  
1018  
1019  
1020  
1021  
1022  
1023

1024  
1025



1026  
1027  
1028

Engel et al., Figure 8